UMEÅ UNIVERSITY

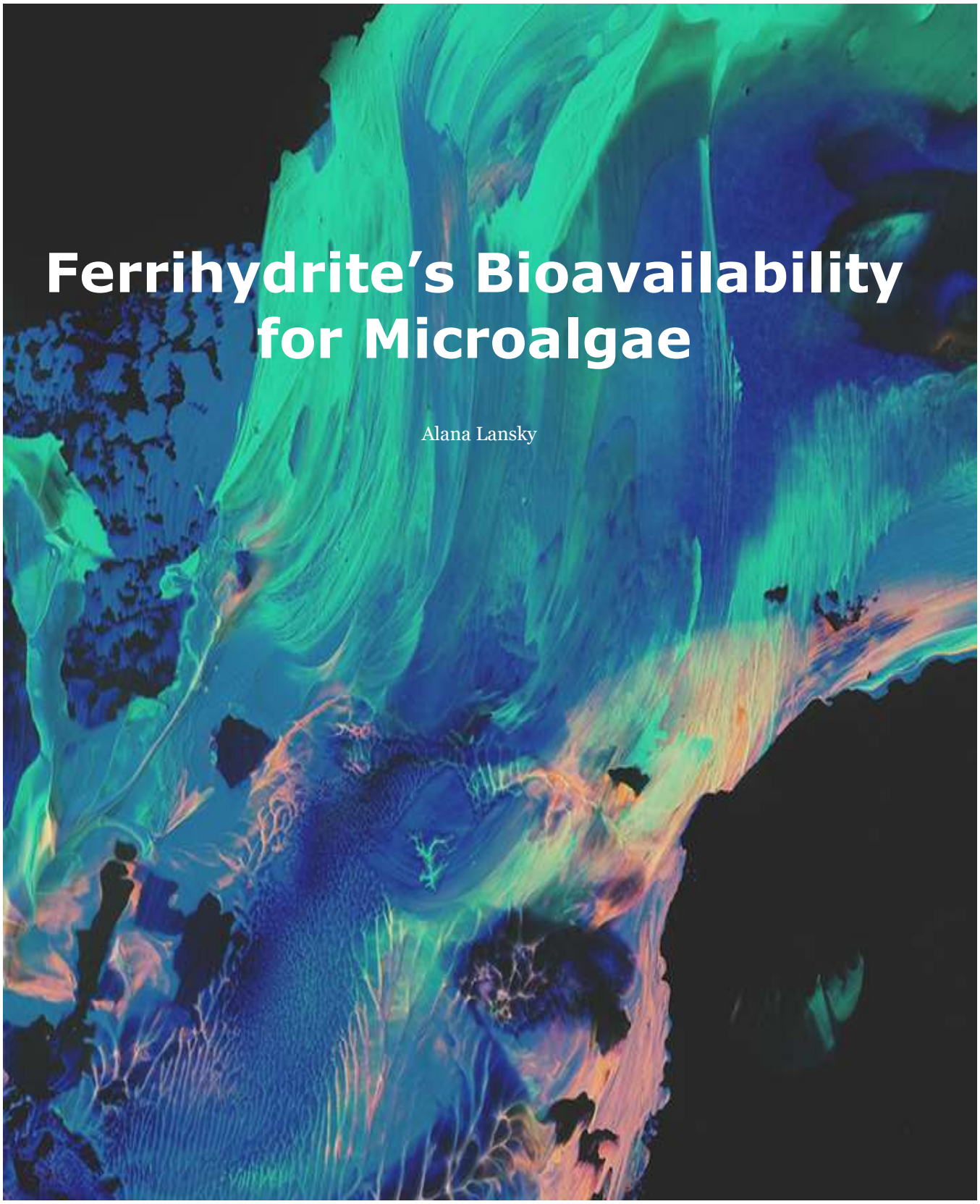

Ferrihydrite's Bioavailability for Microalgae

Alana Lansky

Master thesis, 60 hp
Examiner: Gerhard Gröbner
Passed: 24-01-2024

Abstract

Microalgae play a crucial role in the Earth's ecosystem in addition to being utilized by various industries as a raw material for production of valuable goods. This prompts the question of how their growth conditions can be optimized. This work focuses on one of the crucial nutrients they need in order to grow and live - bioavailable iron. However, in natural open water most of the iron remains in a less soluble form, such as nanoparticulate ferrihydrite. The effects this specific iron oxide has on growth of *Chlorella vulgaris*, a freshwater unicellular green alga, have been compared to those of other forms of iron. The topic of bioavailability has further been tested using different organic agents, which have been shown to facilitate and improve uptake, the focal point being leonardite humic acid (LHA). Growth of *C. vulgaris* has been analyzed using spectrophotometry and cell count, however, the differences between various forms of iron and organic agents have mostly been determined statistically insignificant. Physical and chemical properties of ferrihydrite and LHA (such as iron content, surface charge and particle size) have been examined using XPS, DLS and FTIR. Zeta potential measurement by DLS has showed that ferrihydrite particles are positively charged at biological pH range, as opposed to the negative charge on the surface of microalgae.
ICP-OES analysis has shown that the binding between ferrihydrite and microalgae or LHA occurred within several hours. These analytical methods have allowed a better understanding of the interactions between microalgae, ferrihydrite and LHA in a solution. These interactions require further investigation, especially in cold-adapted species.

Popular Scientific Summary, Societal and Ethical Aspects

Popular scientific summary

Microalgae are water-dwelling organisms that use light, carbon dioxide, and nutrients to produce oxygen and sugar. About 80% of the available oxygen on Earth is produced by algae. They also serve as the primary food source for other marine organisms and are in fact the basis of the marine food chain, without which the marine life cannot survive. For these reasons it is important to investigate what factors affect microalgae growth in oceans.

The focus of this work is one of the nutrients important for microalgal growth, iron. Iron is an element found in oceans in different forms – it can be either dissolved in water or in a form of undissolved particles. Only dissolved iron is available for consumption by microalgae, and it can be bound to organic or inorganic molecules. More than 90% of all dissolved iron in the ocean is bound to organic molecules.

The most interesting to us is one form of iron that is present in oceans – ferrihydrite. It is an important natural nanomineral of the iron oxide family. This project is aimed to explore the availability of ferrihydrite to microalgae for growth and to investigate how exactly this form of iron binds to the surface of the microalgae cell. We hypothesized that ferrihydrite will be more bioavailable to microalgae than other iron oxides, due to its instability in water. Instability will result in faster dissolution, which will allow microalgae to adsorb the former more efficiently than the latter.

In order to test our hypothesis, we used *Chlorella vulgaris* (13-1), a freshwater green microalga. By tracking growth of microalgae cultures over the course of 9-10 days and comparing growth rates, we deduced, which form of iron affected growth the most. Size and surface charge of e ferrihydrite particles have been determined using dynamic light scattering (DLS) and the results were used to discuss the effect of those properties on bioavailability. The iron content of leonardite humic acid (LHA), an organic compound that is found to increase bioavailability of iron, was analyzed using ICP-OES.

Societal aspects

This research project is connected to a broader topic of investigating factors affecting growth of microalgae and can be viewed in the context of the UN Sustainable Development Goals, specifically Goals 13, 14 and 6[1].

Microalgae are the base of the marine food chain, serving as energy source for all higher forms of life. They play a crucial role as consumers of CO_2 and producers of oxygen, which is necessary to sustain life on land and in water. Uptake of CO_2 by microalgae can be used to mitigate the effects of increasing CO_2 emissions and ocean acidification on global warming[2], which is connected to goal 13 (Goal 13 - Climate action).

Health of marine ecosystems (Goal 14 – Life below water) can be affected by changes in growth rates of microalgae, for example harmful algal blooms. One famous case of such harmful effects was the algal bloom of *Chrysochromulina polylepis,* which was reported as a cause of death for approximately 900 tons of fish in the North sea in 1988[3].

Microalgae are used for removal of pollutants, such as heavy metals, from aquatic systems as part of remediation efforts[4]. This illustrates microalgae contribution to Goal 6 (Clean water and sanitation).

It is our duty as environmental scientists to investigate and explore changes that occur in the natural ecosystems that we rely upon, if not for the sake of the biota itself (which is a cause usually perceived as less important than human-related causes), then for the sake of our own demographically growing mankind that is relying upon dwindling resources.

Ethical aspects

This project included no work with animals, human material, human subjects, or GMO. A native species of microalgae has been used for experiments. No new potentially harmful substances have been synthesized during the course of this project.

The raw data is available and has not been altered during data analysis. This goes hand in hand with the ethical norms of the scientific community, to present data objectively and take responsibility for the obtained results. Statistical tools (t-test, ANOVA and Tukey's test) have been utilized to determine significance of results. An effort was made to describe all the experiments as precisely as possible to allow for reproducibility by fellow scientists, to comply with the principle of transparency.

Since this was a practical project, rather than a purely theoretical one, some disposable tools and materials were used, which is inevitable in chemistry lab projects. However, an effort was made to minimize the amounts of disposable resources, while keeping such features as the usage of biological replicates since this is one of the cornerstones of proper scientific experiments. All waste was discarded according to university policy to prevent pollution of wastewater with hazardous compounds and further leaking of those compounds into soil and natural bodies of water.

List of Abbreviations

ANOVA	Analysis of variance
CA	Citric acid
CPS	Counts per second
DLS	Dynamic light scattering
EDTA	Ethylenediaminetetraacetic acid
FH	Ferrihydrite
FTIR	Fourier Transformed Infra-Red (spectroscopy)
Hem	Hematite
HSD	Honestly significant difference
ICP-OES	Inductively coupled plasma optical emission sprectroscopy
IHSS	International humic substance society
LHA	Leonardite humic acid
LOD	Limit of detection
MQ	Milli-Q ultra-pure water
NADP+	Nicotinamide Adenine Dinucleotide Phosphate
NC	Negative control
NOM	Natural organic matter
NORCCA	Norwegian culture collection of algae
NP	Nanoparticles
OD	Optical density
PC	Positive control
PSII	Photosystem II
PZC	Point of zero charge
QY	Quantum yield
SE	Standard error
UV-Vis	Ultra-violet visible (spectroscopy)
XPS	X-ray photoelectron spectroscopy

Author Contribution

ICP-OES measurements have been performed by Martin Plöhn. FTIR measurements have been performed by Jean-Francois Boily. Zeta potential and size particle measurements have been performed by Tao Chen. XPS analysis has been performed by Andrey Shchukarev. All other experiments, measurements and data analysis have been performed by the author.

Table of contents

1.Introduction

Microalgae, unicellular fresh or seawater phytoplankton, have been the focus of increasing scientific interest in the past decades, due to their roles in the Earth's ecosystem as an important part of the aquatic food chain, a consumer of CO_2 and producer of oxygen; their biomass is a valuable feedstock for the production of biofuels, biofertilizer and high value products such as health supplements and cosmetics[5]. As photoautotrophic species microalgae thrive in the presence of light, CO_2 and nutrients[6]. In addition to being present in sufficient concentrations, nutrients also need to be bioavailable, i.e. in a form that is ready for uptake by microalgae cells. In natural environments, specifically in the oceans, the limiting nutrient for growth often is iron[7], an important cofactor for many cellular enzymes (for example, NADP(+) reductase[8]). Bioavailability of iron is affected by its chemical species, mineral phase, solubility, and presence of organic ligands.

In aquatic systems, different types of iron can be found - either in the form of dissolved species complexed to organic (e.g. siderophores) or inorganic (e.g. ferrous hydroxides) ligands, as well as mineral (nano)particles. Two of the most common oxidation states are observed as ferrous iron (Fe^{2+}) and ferric iron (Fe^{3+}). Ferric iron is formed when ferrous iron is exposed to oxidizing conditions, such as O_2 and/or UV radiation[9]. Due to relatively high levels of oxygen, ferric iron is the most common oxidation state to be found in oceans. The different species of iron are characterized by different solubility constants, which play an important role in bioavailability for microalgae, affecting the growth conditions; the more soluble species are, the more bioavailable to microalgae and vice versa[10]. Solubility in seawater can be affected by several factors such as temperature, pH, and salinity[11]. The most common forms of iron in the ocean are characterized by low solubility, making them less available for uptake by microalgae.

The focal point of this work is ferrihydrite ($Fe_5O_8OH•4H_2O$ or $Fe_{10}O_{14}(OH)_2$), a disordered crystalline form of nanoparticulate iron oxyhydroxide. This mineral phase is thermodynamically unstable and therefore transforms with time as a result of oxidizing reactions into more stable and crystalline ordered mineral phases, such as hematite (Fe_2O_3) and goethite (α-FeO(OH)). Out of all iron oxides, ferrihydrite's instability makes it the most likely source of ferric iron for microalgae in the oceans[12].

The presence of organic chelating agents affects the bioavailability of iron to microalgae as well. This occurs when the iron is complexed to an organic molecule, followed by reduction of complexed ferric iron to more bioavailable ferrous iron by ferrireductase. Siderophores, compounds secreted by bacteria present in the same environment as microalgae, represent one such type of organic molecules, which are characterized by high affinity towards ferric iron and the ability to produce iron ions as a result of redox reactions with insoluble forms of iron[10].

In natural waters there are different types of dissolved organic matter, which act as chelating agents, among them are humic acids. Humic acids contains both hydrophilic and hydrophobic functional groups (such as carboxylic and phenolic), which participate in a variety of reactions, for example interactions with metals[13]. Leonardite humic acid (LHA) was chosen for this work for this work to test how organic matter affects the bioavailability of different iron species. In these experiments I used an optimized growth medium (BG11) intended for microalgae, which includes the organic compounds EDTA and citric acid, as well as iron pre-complexed with citrate (ammonium ferric citrate)[14] in order to increase the bioavailability of iron. Three microalgae species were used in this project. *C. vulgaris* (13-1) is a Nordic freshwater unicellular green microalga

characterized by spherically shaped cells, size varying between 2-10 µm and high adaptability to various changes in its environment[15]. Due to its resistance and rapid growth rate, *C. vulgaris* is one of the most common freshwater algae found in Sweden. The Nordic strain 13-1 is adapted to ambient temperatures around 15°C. *Pyramimonas* sp. (UIO 569, obtained from NORCCA[16]) is a marine green alga from the Barentz sea, adapted to 4°C and characterized by pyramidal shape and several flagella. *G. theta* is a marine cryptophyte alga (CCMP2712, obtained from the Bigelow National Center for Marine Algae and Microbiota). Other species of cryptophytes have been found in the Antarctic[17], which prompted the question whether *G. theta* can grow in similar temperatures as well and allow us to explore iron uptake in cold conditions.

Aim of the exam work

The aim of this thesis was to explore how the presence of different types of iron (and different concentrations of those species) affects the growth of the three species of microalgae, *C. vulgaris, G. theta* and *Pyramimonas* sp. The focal point of this project was growth in the presence of ferrihydrite.

Objectives

- Identification of iron forms that promote microalgal growth rates.
- Testing LHA's ability to increase bioavailability of iron.
- Characterization of ferrihydrite nanoparticles in aqueous solutions.

Hypothesis

Iron bioavailability to microalgae is affected by its type, solubility, and presence of organic ligands. Crystalline structures of iron are less bioavailable for microalgae, ferrihydrite therefore should be more bioavailable than hematite due to its less ordered structure. Ferrous iron will be more bioavailable than ferric iron due to the former's higher solubility. LHA present in the microalgae solution will promote growth due to its organic content. Larger size of nanoparticle aggregates will delay growth, since larger particles are less bioavailable.

2. Materials and Methods

2.1 Preparation and cultivation of microalgae cultures

Chlorella vulgaris[18] has been chosen to analyze the effect of ferrihydrite on microalgal growth in the presence of LHA. Two additional cold-water adapted strains were chosen to investigate iron uptake under Arctic conditions - *Pyramimonas* sp.[19] and *Guillardia theta*[20].

C. vulgaris pre-inoculum, previously isolated in the Funk lab and kept in BG11, was used to start all the cultures by adding 1-2 mL to a total final volume of 80 mL. Cell count of the pre-inoculum was determined using Multisizer 3 (as detailed in Section 2.4) which ensured approximately even concentrations of cells among experimental flasks. Experiments were carried out using 250 mL Erlenmeyer flasks that were washed (Lab500 SCL, Steelco) and sterilized (Laboklav - sterilized at 134ºC for 15 min) prior to use. About 80 mL of final solution volume was added to each flask. The inoculation and mixing of components for each setting was performed under laminar flow and so were subsequent daily sampling procedures. The aim of sterilizing flasks and using a hood with a laminar flow was to minimize the chance of introducing contaminations to the cultures.

A modified version of BG11[14] (sterilized at 121ºC for 20 min) was used based on the results obtained previously in the Funk lab, which showed that half the amount of phosphate mentioned in preparation instructions for BG11 is sufficient to sustain growth for an experiment that lasts 10 days. After preparation, flasks were placed into a shaker incubator at 18 ± 2°C, 100 rpm under continuous light intensity of 80 µmol $m^{-2}s^{-1}$, in order to provide gentle stirring of the cultures under light conditions that were found to be optimal for this strain[21].

50 mL Erlenmeyer flasks (washed and sterilized) and 150 mL culture flasks were used for experiments with *Pyramimonas* sp. H/2 medium[22] was used for cultivation. 1L culture flasks were utilized during experiments with *G. theta* and a modified F/2 medium[22] was used for cultivation. For both species of microalgae, flasks were placed in a shaker incubator at 4 ± 2°C at 50 rpm and continuous light intensity of 20 µmol $m^{-2}s^{-1}$.

2.2 Experimental design

Each experiment was designed to have one dependent variable, one or two independent variables and the rest were controlled variables. The dependent variable was growth of microalgae, as observed by several analytical methods (described in detail below). The independent variables were species of iron, concentration of iron and type of organic chelating agent. All growth experiments were carried out using biological triplicates to account for possible variation in the results.

2.2.1 *Chlorella vulgaris*

To analyse the effect of different mineral species of iron (and their concentrations) on growth of *C. vulgaris* conditions of these substances were varied. Positive and negative controls were included in each experiment to verify that microalgal growth indeed occured in standard conditions and accelerated or delayed in dependence to the independent variables.

Growth in the presence of ammonium ferric citrate green (used as a positive control) was compared to ferrihydrite, hematite, or $FeCl_2$. In negative control cultures no iron was added to the culture medium. Ferrihydrite (0.032 M) and hematite (0.0157 M) solutions were synthesized in the Boily lab.

To analyse whether the type of organic matter affects growth, $3.4x10^{-7}$ M EDTA (ethylenediaminetetraacetic acid), $3.12x10^{-6}$ M citric acid or 5% (v/v) leonardite humic acid (LHA) were added to the culture medium. LHA stock solution was prepared by dissolving 2 g of LHA powder (IHSS standard 1S104H) in 100 mL NaOH 1M, and adjusting the volume to 1 L with MQ[23]. The carbon content of the above mentioned solution is 1276 mg L^{-1}, as has been previously determined[23]. The effect of LHA on growth was analysed by growing microalgae in an iron-depleted BG11 in the presence or absence of LHA.

2.2.2 *Guillardia theta* and *Pyramimonas* sp.

G. theta was placed in culture flasks, whereas *Pyramimonas* sp. culture was divided between culture flasks and Erlenmeyer flasks to test whether the type of container affects growth. Growth was observed under limiting light conditions and cold temperature, as specified above. Cells were counted on day 0 and day 10. Since no growth was detected in both species, all the experiments described below were performed using *C. vulgaris*.

2.3 Optical density (OD)

OD was measured at the wavelengths 530, 680 and 750 nm at least every other day using a T-90 UV-Vis spectrophotometer (PG Instruments Ltd) and polystyrene cuvettes (Sarstedt).

With spectrophotometry either absorbance or transmittance of light by a given sample can be measured. A beam of light is shot through the cuvette that contains the sample and a detector located on the other side of the cuvette determines how much of the light passed through the sample. Based on the content of the sample, different chromophores (molecules that absorb certain wavelengths of visible light and reflect others resulting in the molecule´s color) will absorb different wavelengths of that light if the frequency of their vibrations or the differences in energy between electronic energy states coincide with the frequency of the beam of light that hits the sample. The transmittance of the sample is expressed in percentage – 0% is a sample that absorbed all the light and 100% is a completely transparent sample. The transmission value is used as conversion between the absorbance of a chromophore and its concentration in a solution (based on Beer-Lambert's law, Equation 1) with absorbance is calculated as -log[transmission][24].

$$A = \epsilon * c * l \qquad \text{(Equation 1)}$$

Prior to each measurement the instrument was calibrated using a blank suitable for this specific setting, to avoid absorption of other components in the solution than microalgae cells (for example, prior to measuring absorbance of microalgae solutions that contained LHA, a blank made of LHA and BG11 was used).

2.4 Cell count

Microalgae cells were counted at least every other day using a Multisizer 3 (Beckman Coulter). This instrument provides number of cells in the culture per 1 mL by using the Coulter principle – a solution containing the particles (in our case, cells) passes between two electrodes that have a weak constant electric current between them. Passage of particles in the space between the electrodes results in a small change in the electric current and that change can be converted into number and size of particles[25]. In addition to number of cells mL^{-1}, the report provided by the Multisizer software (version 3) includes size distribution of cells in each measurement.

2.5 Quantum yield (QY) and pH

QY was measured every other day using an Aquapen fluorometer (Aquapen-C, Photon System Instruments) and a polystyrene cuvette with 4 clear sides (VWR). This measurement provides general information regarding the overall health of the Photosystem II protein complex, which is responsible for the water oxidation step in the photosynthetic process. QY values of 0.7 - 0.8 are expected in a healthy culture and point to higher efficacy of PSII[26], whereas relatively lower values indicate more PSII sites are damaged and the health of the cells is deteriorating[27]. Prior to measurements, samples were dark adapted for at least 30 min.

As another indicator of the overall health of the culture, pH was monitored every other day using a pH meter (VWR). The pH of BG11 is around 7, lower pH values measured as the experiment progresses might indicate there is bacterial overgrowth in the flasks.

2.6 Growth rate

Exponential growth rate (μ_{exp}) calculation is a quantitative way to compare microalgal growth and reach conclusions regarding the stimulating or limiting effect of different types of iron (or other changing conditions). In all experiments the growth rates of the

exponential phases were calculated by using cell count values both in Excel (Equation 2[28]) and Prism (using the exponential growth model[30]).

$$\mu\left(\frac{divisions}{day}\right) = \frac{LnB_N - LnB_0}{t_N - t_0} \quad \text{(Equation 2)}$$

Where B_0 is microalgal density at first day of exponential phase, B_N is microalgal density at last day of exponential phase and t_N-t_0 is number of days in exponential phase.

2.7 ICP-OES

ICP-OES (Inductively coupled plasma – optical emission spectroscopy) is an analytical method used to determine the elemental composition of a given sample. It works by first turning a liquid sample into aerosol and using high-temperature plasma to ionize the components of the sample. In the process of ionization, the electrons in the different elements that compose the sample become excited and transition to higher energy states. After some time, the electrons relax to lower energy states and in the process of relaxation the excess energy is emitted as photons. The emission occurs in different wavelengths that are unique to each element, creating a "fingerprint" of that element that allows the instrument to identify the different elements that compose the sample. The output includes a quantification of the concentration of specific elements in the sample[31]. A specific element in a sample can be detected using several wavelengths in which the element emits photons.

Measurements were performed using ICP-OES 5800 (Agilent Technologies) with argon as a carrier gas, and the intensity of iron was measured at 238.204 nm[32]. Prior to measurements, it is necessary to measure a series of standards, i.e., solutions with known concentrations that form a calibration curve which is used to convert the output (intensity) to concentration. The estimated concentration in the sample needs to fall within the lowest and highest concentrations of standards, otherwise the results are invalid.

Iron standards for ICP-OES were prepared by dissolving $FeCl_3$ in nitrified MQ, in concentrations ranging from 20 mmol L^{-1} to 0.02 fmol L^{-1}. A purchased iron standard kindly provided by Erik Björn (TraceCERT, 1 g L^{-1} in HNO_3) was used as well.

Microalgae samples were prepared for analysis by first filtering them using 0.22 µm sterile hydrophilic filters (Sarstedt) in order to remove larger particles from the solution (mainly microalgae cells and larger particles of LHA). The remaining liquid was acidified using HNO_3 65% and nitrified water (1% of HNO_3 65% in MQ) to prevent precipitation of insoluble iron oxides. Standards and samples were stored in a cold room (4 ºC) until testing.

LHA dry powder sample was prepared for analysis of iron concentration by acid digestion. It was necessary to modify the method of digestion using aqua regia[33] due to logistical reasons. Therefore, 1 M HCl (made from HCl 37% by VWR) was added to the sample and allowed to stand for 24 hours at room temperature (20 □C). This was repeated on a new sample with 12 M HCl (made from HCl 37% by VWR) and the results were compared.

The order of steps during sample preparation for ICP-OES analysis (filtering and acidification) was tested to see whether it affects the results by preparing samples both ways and measuring the iron concentration. A t-test was done to determine whether the difference between the concentration values is significant.

2.8 Characterization of ferrihydrite nanoparticles - Zeta potential, hydrodynamic diameter, and number of binding sites.

The particle size and zeta potential of ferrihydrite have been measured using Zetasizer (Malvern). This instrument works according to the DLS (dynamic light scattering) principle, which states that particles in a solution will move according to Brownian motion, meaning randomly (unless there are other forces that impact them, such as an electric field or gravity). When particles move, they collide with the solvent molecules and their kinetic energy changes because of those collisions. Larger particles move slower compared to smaller particles. When a beam of light passes through the colloid suspension, the photons hit the particles and get dispersed. This dispersion forms a different pattern which changes as a result of the particle movement. The pattern changes quicker if the particle is smaller and vice-versa, which allows to calculate their hydrodynamic diameter[34].

Zeta potential (measured in mV) is a value that essentially represents the electrostatic potential at particle surfaces, which can be either negative or positive. High surface potential will lead to more repulsion between the particles and thus, a more stable colloid suspension. Low surface potential that decreases until the point of zero charge will lead to more attractive forces between the particles resulting in aggregating (since it lowers the surface energy and therefore is more thermodynamically favorable). In this case, the size that will be measured by the instrument will be the size of the particle cluster and not a single nanoparticle. Zeta potential is affected by pH and ionic strength, which need to be monitored during measurements.

A suspension of ferrihydrite nanoparticles was analyzed using the Zetasizer in a range of 6.0 – 9.0 pH in order to determine the point of zero charge. During this analysis the hydrodynamic diameter of nanoparticles was measured as well.

The number of binding sites on nanoparticles can be estimated using Equation 3[35]. In this project it was used to calculate the theoretical number of binding sites on ferrihydrite.

$$Conc.\left(\frac{mol}{L}\right) = M_S * S_A * \rho * \frac{1}{N_A} \qquad \text{(Equation 3)}$$

Where M_S is the density of nanoparticle suspension (g L^{-1}), S_A is the specific surface area of nanoparticle (m^2 g^{-1}), ρ is the density of binding sites (sites nm^{-2}) and N_A is Avogadro's number.

2.9 XPS

XPS (X-ray photoelectron spectroscopy) analysis is based on the photoelectron effect, where X-rays hit a sample and cause the release of electrons from the atoms on the surface. The kinetic energy of the emitted electron is correlated with the depth from which this electron was released. Measuring the kinetic energy of those electrons and plotting it results in a spectrum where peaks can be identified and attributed to an electron from a certain orbital in an element, thus identifying the element[36]. The resulting spectrum is comprised of peaks created as a result of photoelectrons emission and Auger photoemission peaks.

XPS analysis using Electron spectrometer Axis Ultra DLD (KRATOS Analytical. Ltd) was performed by Andrey Shchukarev on a sample of microalgae solution that contained added ferrihydrite after the sample was air-dried at room temperature. This method was also used to analyze the surface of dry LHA powder for presence of iron.

2.10 Glassware preparation

Three different methods were compared – dishwasher only, dishwasher followed by washing three times with MQ and dishwasher followed by an acid bath[37] followed by washing three times with MQ. All flasks were sterilized after cleaning and used for incubation of microalgae in identical conditions (same composition as positive control). Optical density was measured on days 0 and 6, to assess whether there were significant differences between the growth of microalgae in differently treated flasks.

2.11 Statistics, literature search and AI usage.

Diva portal, Google Scholar, and Sci-Finder were used for literature search. All growth experiments have been performed in triplicates, using biological replicates, unless stated otherwise. For statistical purposes it was necessary to calculate standard error (SE, a measure of how accurately the mean of the samples represents the mean of the population) values to be used as error bars. The data is expressed in mean ± SE (n = 3), except when stated otherwise. Statistical analysis was done using one-way ANOVA in the case of experiments with one independent variable and two-way ANOVA in experiments with two independent variables. If the p value of ANOVA was smaller than 0.05, Tukey's test was performed on individual pairs of treatments. SE calculations, ANOVA and Tukey's test were done using Excel (Office 365). Plots were fitted using Excel and specific growth rates were calculated using Prism (GraphPad, version 10.1.1). AI was not used for the purpose of writing this report.

3. Results

3.1 Appearance of *Chlorella vulgaris* cultures

Some of the flasks containing *C. vulgaris* were observed to develop a ring of aggregated microalgae cells right above the solution level in the flask (**Figure A1.1**). The ring was gently scraped using an inoculation loop every day prior to sampling.

During microalgal growth often aggregation at the side of the culture flasks was observed. Therefore, cleaning methods of Erlenmeyer flasks were compared to determine whether a different method can prevent these aggregations.

Three cleaning methods of flasks were compared by measuring algal growth (OD_{680} on day 0 and day 6 of incubation, **Figure A1.2**). The physical appearance of the cultures was also recorded, i.e. the appearance of flocculation or cell aggregation (**Figure A1.3 A-C**). Regardless of the cleaning method, aggregation of the microalgae was observed in all flasks. On day 0 the OD was measured to be 0.140 in the flask treated with dishwasher only, 0.134 in the flask washed with deionized water (MQ) after dishwashing and 0.136 in the flask washed with acid bath and MQ after dishwashing. The OD on day 6 of culture growth was measured to be 0.421 in the flask treated by dishwasher only, 0.387 in the flask treated by dishwasher and MQ and 0.402 for dishwasher followed by an acid bath and MQ.

3.2 Growth rates and overall health of *Chlorella vulgaris* cultures containing various types of iron and organic agents.

To analyse growth stimulation of various species of iron, cultures of *Chlorella vulgaris* (13-1) were grown in BG11 depleted of iron (negative control), or in the presence of either 23 μM ferrihydrite, 23 μM hematite or 0.015 μM $FeCl_2$. Addition of 23 μM ammonium ferric citrate green, which is present in regular BG11, served as a positive control (**Figure 1**). Positive control cultures were the only ones that contained 3.12×10^{-6} M citric acid and 3.4×10^{-7} M EDTA as organic agents (standard components of BG11). All cultures were inoculated with ~1×10^6 cells mL^{-1} on day 0, however, after 10 days of

growth the positive control exhibited the highest final count of 43.43 ± 0.32x10^6 cells mL^{-1}, followed by the cultures containing $FeCl_2$ (36.59 ± 3.07x10^6 cells mL^{-1}) and ferrihydrite (20.64 ± 0.69 x10^6 cells mL^{-1}). Both hematite and the negative control showed relatively minor growth with a final measurement of only 8.40 ± 0.29x10^6 cells mL^{-1} and 9.77 ± 0.16x10^6 cells mL^{-1}, respectively.

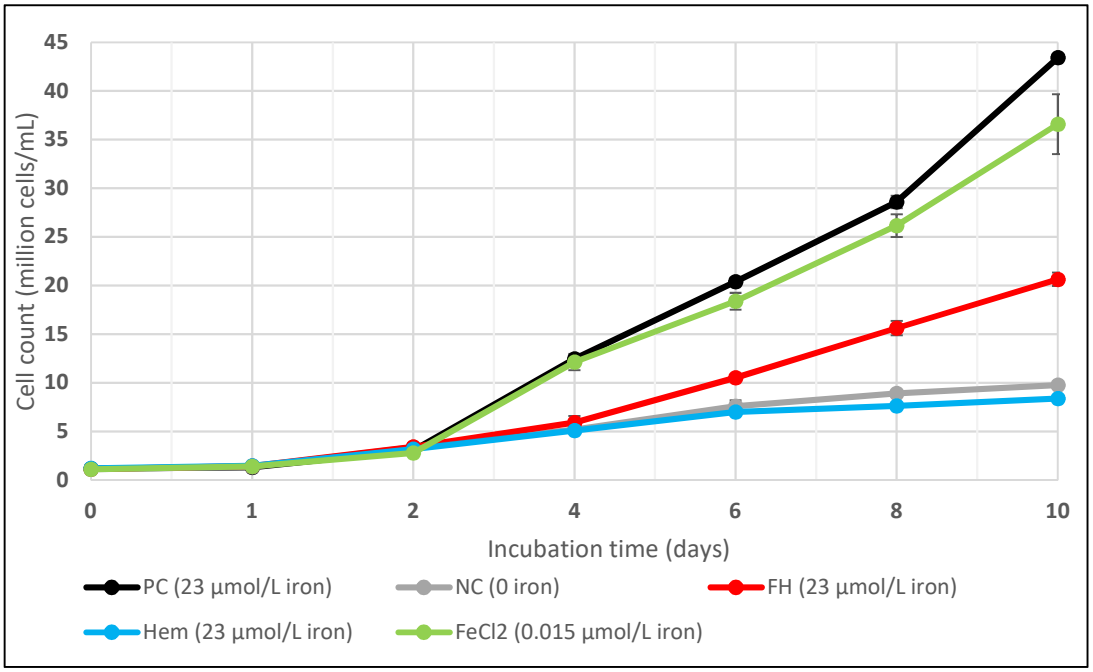

Figure 1. Availability of different iron species for the growth of *C. vulgaris*. Positive control (PC, 23 µM ammonium ferric citrate green + 3.12x10^{-6} M CA + 3.4x10^{-7} M EDTA), negative control (NC, iron-depleted), ferrihydrite (FH 23 µM), $FeCl_2$ (0.015 µM) and hematite (Hem, 23 µM). Mean values ± SE (n = 3) are presented. Calculated p value = 2.5x10^{-8}

Exponential growth rates (**Figure A1.4**) have been calculated based on cell count values presented in **Figure 1**. While addition of 23 µM ammonium ferric citrate green (positive control, PC) resulted in a growth rate of 0.386 day^{-1}, depletion of iron (negative control, NC) resulted in a growth rate of only 0.217 day^{-1}. Addition of 0.015 µM $FeCl_2$ to the cultures induced a growth rate of 0.363 day^{-1}, 23 µM ferrihydrite 0.291 day^{-1} and 23 µM hematite 0.199 day^{-1}.

Measurements of pH in these cultures (**Figure A1.5**) at day 0 indicated pH values between pH 7-8 (23 µM hematite pH 8.10; 23 µM ferrihydrite pH 7.54, $FeCl_2$ pH 7.40; 23 µM ammonium ferric citrate green as PC pH 7.17 and iron-depleted NC pH 7.06, respectively). At day 1, a decrease in pH was observed in all cultures to values in the range of pH 7.26 - 7.39. After 4 days of growth a pH increase was observed in all cultures, which indicates active photosynthesis of the microalgae. The highest value for the positive control culture was measured already on day 8 (pH 9.92), while the negative control culture as well as the cultures grown in the presence of ferrihydrite, hematite and $FeCl_2$ reached maximal pH values at day 10 (pH 8.43, 9.10, 8.17, 9.93, respectively).

After growth of *C. vulgaris* was established in the presence of ferrihydrite, the stimulating effect of different types of organic ligands (3.12x10^{-6} M CA, 3.4x10^{-7} M EDTA or 5% (v/v) LHA was investigated (**Figure 2**). Cultures were inoculated with around ~1x10^6 cells mL^{-1} on day 0, and growth of the cells was investigated for 10 days. Highest cell count was observed in cultures containing 23 µM ferrihydrite and 5% LHA

(13.72 ± 0.20x10^6 cells mL^{-1}), followed by those containing only 23 µM ferrihydrite without any organic agent (9.45 ± 6.36x10^6 cells mL^{-1}) and then those containing 23 µM ferrihydrite + 3.12x10^{-6} M CA + 3.4x10^{-7} M EDTA (4.46 ± 2.57 x10^6 cells mL^{-1}). Both positive (23 µM ammonium ferric citrate green + 3.12x10^{-6} M CA + 3.4x10^{-7} M EDTA) and negative (iron-depleted + 3.12x10^{-6} M CA + 3.4x10^{-7} M EDTA) controls showed relatively lower growth with a final measurement of 3.19 ± 0.80x10^6 cells mL^{-1} and only 1.41 ± 0.19 x10^6 cells mL^{-1}, respectively.

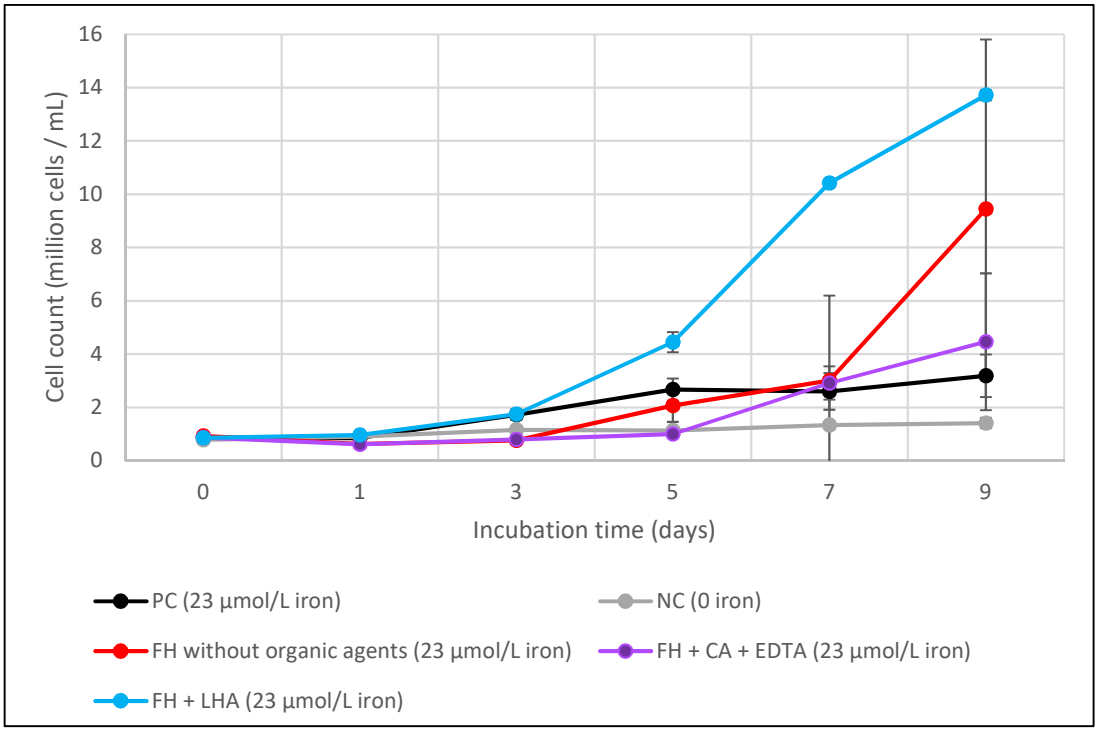

Figure 2. Growth of *C. vulgaris* in the presence of ferrihydrite and different organic agents. Positive control (PC, 23 µM ammonium ferric citrate green + 3.12x10^{-6} M CA + 3.4x10^{-7} M EDTA), negative control (NC, iron-depleted + 3.12x10^{-6} M CA + 3.4x10^{-7} M EDTA), ferrihydrite in the absence of organic agents (FH, 23 µM), ferrihydrite in the presence of citric acid and EDTA (23 µM FH + 3.12x10^{-6} M CA + 3.4x10^{-7} M EDTA, ferrihydrite in the presence of LHA (FH 23 µM + 5% LHA). Mean values ± SE (n = 3) are presented. Calculated p value = 0.03

Exponential growth rates (**Figure A1.6**) have been calculated based on the cell count values presented in **Figure 2**. The culture with 23 µM ferrihydrite and 5% LHA added had the highest growth rate of 0.341 day^{-1}, followed by the culture with added ferrihydrite (23 µM, without organic agents) that had a rate of 0.256 day^{-1}. 23 µM ferrihydrite in the presence of 3.12x10^{-6} M CA and 3.4x10^{-7} M EDTA induced a growth rate of 0.205 day^{-1}. Both positive (23 µM, ammonium ferric citrate green + 3.12x10^{-6} M CA + 3.4x10^{-7} M EDTA) and negative (iron-depleted + 3.12x10^{-6} M CA + 3.4x10^{-7} M EDTA) controls showed relatively lower growth rates of 0.158 day^{-1} and only 0.055 day^{-1}, respectively.

Measuring the pH values of these cultures (**Figure A1.7**) showed that already on day 0, the culture containing 23 µM ferrihydrite and 5% LHA had the highest pH value of 9.46, compared to the other cultures which showed values ranging between pH 6.98 - 7.08. However, the pH value of the culture containing 23 µM ferrihydrite and 5% LHA decreased on day 1 to pH 7.24, on the following days a steady increase in pH was observed, resulting in pH 8.9 at day 9 of the experiment. At day 1, the positive control

(23 μM ammonium ferric citrate green + $3.12x10^{-6}$ M CA + $3.4x10^{-7}$ M EDTA) showed a noticeable decline to pH 6.56, while the other cultures varied between pH 7.07 - 7.46. With the exception of the abovementioned culture containing 23 μM ferrihydrite and 5% LHA, the cultures showed maximal pH values on the last day of measurement, day 9 – the negative control (iron-depleted + $3.12x10^{-6}$ M CA + $3.4x10^{-7}$ M EDTA) had a pH value of 7.70, the cultures in the presence of 23 μM ferrihydrite (with $3.12x10^{-6}$ M citric acid and $3.4x10^{-7}$ EDTA) a pH of 8.47 and the culture containing 23 μM ferrihydrite without organic agents a pH of 8.48.

Quantum yield measurements (**Figure A1.8**) at day 0 resulted in the value 0.63 for the negative control, but also for the culture grown in the presence of ferrihydrite and LHA, for the other cultures the measured value was 0.66. These were the lowest measured values throughout the experiment, indicating that the cultures still were in lag-phase. After three days of growth maximal QY values were measured for all cultures (0.79 for the positive control (23 μM ammonium ferric citrate green + $3.12x10^{-6}$ M CA + $3.4x10^{-7}$ M EDTA) and cultures with 0.015 μM $FeCl_2$ and 23 μM ferrihydrite and 5% LHA present, 0.78 for cultures with 23 μM ferrihydrite in the absence of organic agents). The negative control (iron-depleted + $3.12x10^{-6}$ M CA + $3.4x10^{-7}$ M EDTA) had a maximal QY of 0.66 at day 2.

Microalgal growth has also been measured (**Figure 3**) in a set-up designed to test the effect of the organic agent LHA when combined with different species of iron (5% LHA was added to all cultures except for positive control and negative control). At day 0, all cultures contained ~$1x10^6$ cells mL^{-1}. After 10 days of growth, however, there was a drastic difference observed in cell number between the cultures that contained LHA compared to those depleted of LHA. The positive and negative controls contained 3.630 ± $0.258x10^6$ cells mL^{-1} and 1.279 ± $0.097x10^6$ cells mL^{-1}, respectively. In the presence of 5% LHA at day 10 all cultures contained more than ~$6x10^6$ cells mL^{-1}. The highest count was measured in the presence of 23 μM hematite and LHA and in the presence of the negative control only containing 5% LHA, but no extra iron species (9.638 ± 0.198 $x10^6$ cells mL^{-1} and 9.373 ± 0.716 $x10^6$ cells mL^{-1}, respectively). The presence of 0.15 nM ferrihydrite and 5% LHA resulted in a cell count of 8.931 ± $0.609x10^6$ cells mL^{-1}. A culture with 23 μM ferrihydrite in the presence of 5% LHA had the lowest cell number among the cultures that contained LHA of 6.931 ± $0.183x10^6$ cells mL^{-1}. Statistical variation of the cultures is shown in supplementary material (**Figures A1.9-A1.11**).

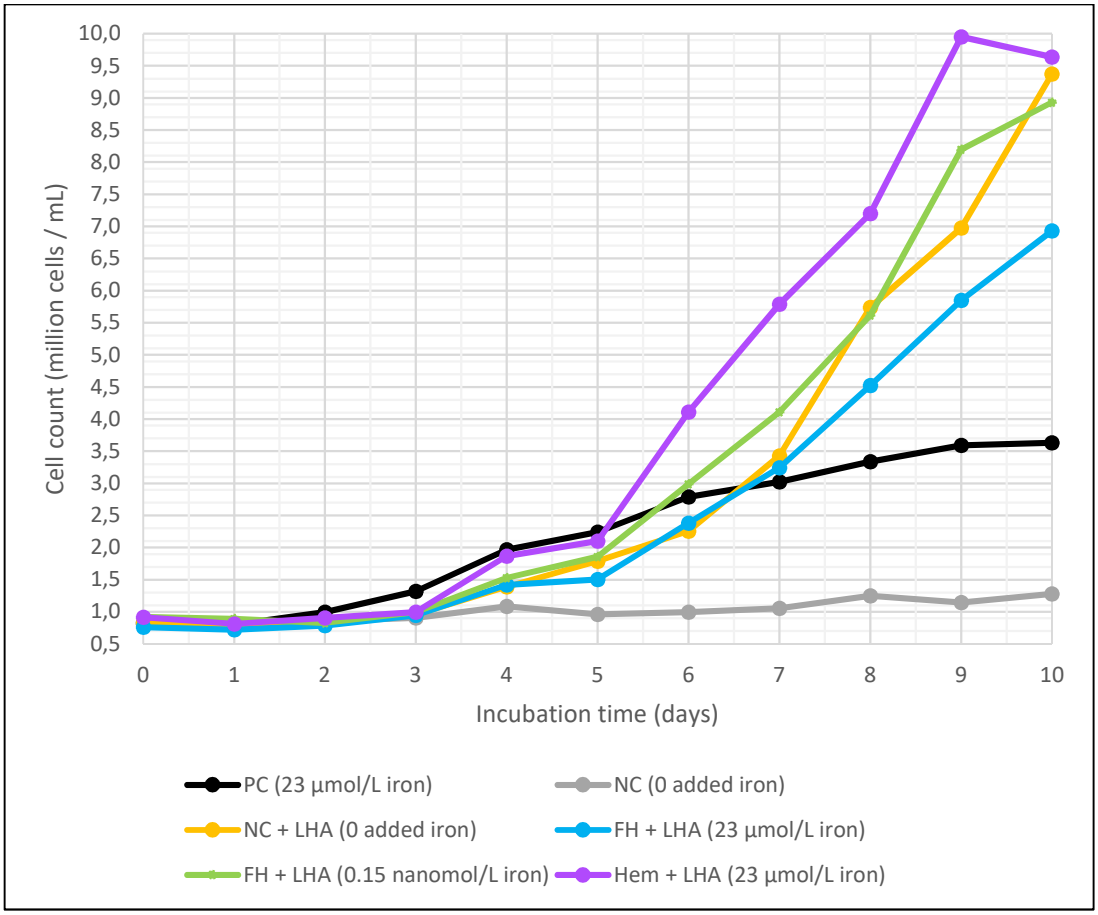

Figure 3. Cell number in cultures of *C. vulgaris* containing LHA and varying species and concentrations of iron. Positive control (PC, 23 µM ammonium ferric citrate green + $3.12x10^{-6}$ M CA + $3.4x10^{-7}$ M EDTA), negative control (NC, iron-depleted + $3.12x10^{-6}$ M CA + $3.4x10^{-7}$ M EDTA), negative control containing LHA (NC + 5% LHA), ferrihydrite (23 µM) with LHA (FH + 5% LHA), ferrihydrite (0.15 nM) with LHA (FH + 5% LHA), and hematite (23 µM) with 5% LHA (Hem + LHA).
Mean values (n = 3) are presented. P value = $2.64x10^{-7}$

Exponential growth rates (**Figure A1.12**) have been calculated based on cell count values presented in **Figure 3**. The highest exponential growth rates were observed for cultures containing cultures containing 5% LHA, with a rate of 0.294 day^{-1} for cultures containing 23 µM hematite and LHA, followed by 0.270 day^{-1} for cultures containing negative control and LHA. The growth rate of the culture containing 0.15 nM ferrihydrite and LHA was calculated to be 0.267 day^{-1} and the rate of the culture with 23 µM ferrihydrite and LHA was 0.251 day^{-1}. The positive (23 µM ammonium ferric citrate green + $3.12x10^{-6}$ M CA + $3.4x10^{-7}$ M EDTA) and negative (iron-depleted + $3.12x10^{-6}$ M CA + $3.4x10^{-7}$ M EDTA) controls, in the absence of LHA, showed the lowest growth rates in comparison to the other cultures (0.173 day^{-1} and 0.044 day^{-1}, respectively).

The pH in the cultures (**Figure A1.13**) containing 5% LHA was higher at day 0 (ranging between pH 8.65 - 9.13) compared to the positive (23 µM ammonium ferric citrate green + $3.12x10^{-6}$ M CA + $3.4x10^{-7}$ M EDTA) and negative (iron-depleted + $3.12x10^{-6}$ M CA + $3.4x10^{-7}$ M EDTA) controls (pH 7.35 and 7.12, respectively). At day 1 it decreased in the cultures that contained LHA (pH 7.75 - 7.92), whereas it increased in the positive and negative controls (pH 7.67 and 7.41, respectively). During longer incubations, all cultures showed a steady increase in pH values and on the last day the negative control reached a pH value of 7.62, whereas the other cultures obtained values in the range of pH 8.55 - 8.97.

On day 0 the positive control (23 μM ammonium ferric citrate green + $3.12x10^{-6}$ M CA + $3.4x10^{-7}$ M EDTA) and cultures containing 23 μM hematite and 5% LHA had QY values of 0.62 (**Figure A1.14**), while the negative controls (iron-depleted), independent of the presence or absence of 5% LHA as well as the culture containing ferrihydrite (23 μM) and 5% LHA exhibited QY values of 0.60. Cultures containing ferrihydrite (0.15 nM) and 5% LHA were measured to have QY values of 0.61. As expected, the QY values increased in all cultures on days 1 and 3. On day 3 the positive control reached a maximal value of 0.78, which then decreased until day 9 (QY value of 0.76). QY of the negative control increased until day 5 (0.76) and then declined to a final QY value of 0.66. Also, the negative control containing 5% LHA reached its maximal QY value on day 5, 0.77, and then decreased to a value of 0.75 on day 9. Cultures containing ferrihydrite (23 μM or 0.15 nM) and 5% LHA reached a maximal QY value on day 5 (0.78 and 0.77, respectively), which then decreased to 0.77 and 0.76, respectively. Cultures containing 23 μM hematite and LHA reached maximal values on day 5 (0.77), which decreased to 0.75 on day 9.

3.3 Growth of *Pyramimonas* sp. and *Guillardia theta*

Results of growth experiments with *Pyramimonas* sp. and *G. theta* in 4°C and reduced light intensity (20 μmol $m^{-2}s^{-1}$ compared to 80 μmol $m^{-2}s^{-1}$ in *C. vulgaris* growth experiments) are presented in **Table A1.15** and **Table A1.16**, respectively. Both species of microalgae were placed in a setting aimed to mimic temperature and light intensity in the Arctic, in order to investigate iron uptake and bioavailability in those conditions. The first step in our planned experiment was to place both species under colder temperature and reduced light intensity in medium solutions containing a standard source of iron ($FeCl_3$), to track growth and then to continue to settings with ferrihydrite as an iron source. *G. theta* was placed in culture flasks, while *Pyramimonas* sp. was divided between culture flasks and Erlenmeyer flasks to check whether there is a significant difference in growth between the two types of containers.
However, the results of cell numbers in *Pyramimonas* sp. showed the culture is dying and the cell numbers in the *G. theta* culture were not counted on day 10 at all since the cultures looked like the cells had died (green color was observed, instead of the expected pink-brownish). Therefore, the experiments with those species were not continued.

3.4 Iron content in microalgae cultures and LHA

Several analytical methods were used to assess the LHA standard that was used for experiments, as well as the presence and concentration of iron in the cultures. ICP-OES was used to determine the concentrations of iron during the progression of the experiment to assess how much of the added iron remained in the solution and was not adsorbed or absorbed by the microalgae. It was also used to determine the iron concentration in the LHA standard. FTIR was used to determine the presence of different species of iron in the stock solutions of iron that were used for the experiments and in the algae cultures. XPS was used to investigate whether iron was adsorbed to the outer wall of the microalgae cells and the composition of LHA dry powder. Excel was used for calculations of growth rate and for statistical tests to assess the significance of the results.

ICP-OES measurements to determine the iron concentration in samples showed that a solution that should contain LHA and $FeCl_3$ at a concentration of 23 μM (**Table A2.1**) in fact contained LHA and $FeCl_3$ at a concentration of 20.03 ± 1.80 μM when using method "A" and 18.38 ± 0.21 μM when using method "B". Solutions that contained ferrihydrite and LHA, again at a concentration of 23 μM, the result for method A was 1.68 ± 0.22 μM and for method B 1.54 ± 0.06 μM. For solutions containing hematite

and LHA, the intensity values that were used to calculate concentration were below level of detection for both methods. The concentrations were calculated using the output of the measurements, given as absorption intensity, by using a calibration curve of pre-prepared standards with known concentrations of iron (**Figure A2.2**).

The iron concentrations at day 0 and day 5 in *C. vulgaris* cultures grown in the presence of LHA (**Figure 3)** measured by ICP-OES are shown in **Table A2.3**. The concentrations were calculated by plotting the absorption intensity of the samples in the calibration curve of pre-prepared standards with known iron concentrations (**Figure A2.4**). The positive control was calculated to contain an iron concentration of 19.53 ± 0.15 μM at day 0 and 0.07 ± 0.06 μM at day 5. The culture containing 0.15 nM of ferrihydrite showed a result below level of detection at day 0 and was calculated to contain 1.13 ± 0.11 μM at day 5. The culture containing 23 μM of hematite showed a result below level of detection at day 0 and was calculated to contain 1.8 ± 1.03 μM at day 5. The other samples showed iron concentrations below the level of detection both on day 0 and day 5.

In order to quantify the iron content in LHA, iron was extracted from LHA using two different concentrations of HCl. For a comparison, a control sample of LHA in MQ water was analyzed as well. After the extraction the acid-containing sample appeared to have an orange-red color (**Figure A2.5**). The resulting solutions were filtered and acidified using nitric water and concentrated nitric acid and analyzed by ICP-OES (**Table A2.6**). Only one replicate of each setting was analyzed. The mean value of 1 M HCl extraction results was 1.894 ± 0.400 μM (n = 3).

The measurements of the iron concentrations of LHA in MQ water and using 12 M HCl for extraction were inconclusive. The calibration curve in **Figure A2.4** was used to calculate the iron concentrations of these measurements.

3.5 Characterization of ferrihydrite

XPS analysis (**Figures A3.1-A3.3**) was performed on day 10 of a *C. vulgaris* culture grown in the presence of ferrihydrite (**Figure 3**) and on a sample of LHA powder. The peaks that are characteristic to specific orbitals in elements[38] are marked in both plots and summarized in **Table A3.4**. Peaks marked as KLL are Auger emission peaks. In both spectra, no peaks characteristic for Fe 2p orbital were observed (usually found between 707 - 720 eV).

C. vulgaris cultures containing ferrihydrite either at 23 μM or 0.15 nM were analyzed by FTIR and spectral peaks characteristic for *C. vulgaris*[39] and expected areas for iron oxide[40] have been assigned (**Figure A3.5**). This experiment was performed to confirm that ferrihydrite is present in those cultures and was not transformed to hematite (which can happen with time). The samples were dried prior to analysis and analyzed in the range of wavenumbers 500 - 4,500 cm^{-1}. In all these spectra, no characteristic peaks of iron oxides could be identified. A sample that contained only microalgae solution without iron was analyzed as well.

The concentration of adsorption sites on ferrihydrite particles that were used for our experiments has been estimated to be 2.6 mM (using previously reported values)[35]. This value means that under the assumption there are three adsorption sites per squared nm on the surface of ferrihydrite, in a suspension that contained 2.6 g L^{-1} ferrihydrite, there were in total 2.6 mM adsorption sites in the entire suspension.

Where M_S is the density of the ferrihydrite suspension (2.6 g L^{-1}), S_A is the specific surface area of ferrihydrite (200 nm^2 g^{-1}), ρ is the density of binding sites (3 sites per nm^{-2}) and N_A is the Avogadro constant.

Zeta potential of ferrihydrite nanoparticles was measured to assess the colloidal stability of the microalgae solutions. The particle size was also measured since it has the potential to affect the bioavailability of the nanoparticles.

The zeta potential (**Figure A3.6**) and particle size (**Figure A3.7**) of ferrihydrite were measured using the Zetasizer. Prior to the measurement, the pH electrode of the instrument was calibrated using solutions of pH 4, 7 and 9. The pH was monitored during the measurement to find the point of zero charge (a value of 8.1, taken from a recent publication[41], was used as a reference point).

The ferrihydrite solution was prepared by 10-time dilution of the stock solution Ten measuring points were determined, and each point was measured with three technical replicates. In total, 21 measurements of the zeta potential and 21 measurements of the particle size were performed. The point of zero charge was calculated by the Zetasizer software to be at pH 8.69 (**Figure A3.6**). The ionic strength has been calculated to be 6.72 mM at pH ~7, based on conductivity measured by the Zetasizer.

In addition to the experiments mentioned above, Zeta potential was measured in a culture of *C. vulgaris* (BG11 media, at pH 7.1) in order to determine the surface charge on the microalga cells. This has resulted in a mean value of -28.5 ± 0.64 mV.

An attempt to measure particle size of ferrihydrite in the same solution was not possible due to the concentration of ferrihydrite being too small for this kind of measurement (as indicated by the Malvern software during data analysis). Therefore, a measurement of ferrihydrite hydrodynamic diameter was done on a more concentrated suspension (unknown concentration) of ferrihydrite at pH 6, which resulted in a mean value of 158.80 ± 43 nm.

4. Discussion

The aim of this thesis work was to establish the effect of various iron species on the growth of microalgae. I therefore cultivated *Chlorella vulgaris* in the presence and absence of different iron species and also investigated the effect of organic compounds on the availability and uptake of iron by the microalgae.

4.1 Appearance of *Chlorella vulgaris* cultures

A green ring of aggregated microalgae was noticed in flasks cultures containing cultures of *C. vulgaris* (except for flasks that contained negative control cultures). This ring remained even after rigorous shaking of the flask. The aggregated algae could gently be scraped off by using an inoculation loop prior to each sampling.

These cell aggregates, however, might have influenced the cell counting. This has been partially addressed by parallel measurements of OD where the absorbance is measured regardless of whether the culture exists as single cells or clusters. It should be noted that in the case of aggregate formation, the aggregates will precipitate to the bottom of the OD cuvette, and this can provide inaccurate results about the density as well since one of the assumptions when measuring OD is that the particles are suspended in the

solution[24]. This can be mitigated by starting the measuring as quickly as possible after transferring the solution into the cuvette.

However, the concern remained that aggregating in a form of a ring prevented the adsorbed cells from having the same access to light as the cells that float freely in the solution have[52]. It remains unclear why this ring was observed in some flasks but not in others. It should be mentioned that it has been reported previously that this might happen in cultures where iron is a limiting growth factor[53].

Aggregates of microalgae cells can occur due to changes in the surface charge. Generally, the cells are charged and repel each other but when the charge decreases it can promote aggregation. This can happen for example when negatively charged particles are in the presence of positively charged ions, such as Ca^{2+}, as was shown before[52]. It was decided to try different washing methods (acid bath and washing with MQ prior to use) to see whether an alternative method can prevent this phenomenon. A statistical analysis ($\alpha = 0.05$) has shown that there was no significant difference between the three methods in terms of cell growth. As can be seen in the pictures in Section 3.1, the ring formed on the walls of all flasks.

Zeta potential measurement was also done on microalgae cells to empirically determine their surface charge in our solutions, as detailed in Section 4.4 below.

4.2 Growth rates and overall health of *Chlorella vulgaris* cultures containing various types of iron and organic agents.

Growth of microalgae can generally be divided into stages – lag phase, exponential phase, linear phase, stationary phase, and death phase by plotting cell count numbers or OD against time (**Figure A4.1**). The experiments were carried for 9-10 days to account for measurements to be performed during the lag, exponential and stationary phases for proper assessment of the growth rate.

The growth curve of *C. vulgaris* have been evaluated in three cultures in order to test the bioavailability of ferrihydrite in comparison to other types of iron and in the presence of different organic agents. In nature (e.g. the oceans) iron is a limiting growth factor, however, it has also been shown before that while iron is crucial for promoting and sustaining growth, concentrations that exceed 40 mg L^{-1} (equals to 716 μM of iron) can hinder growth[42]. In all growth experiments in this project, the concentration was about one order of magnitude lower (23 μM).

The general appearance of all cultures shared a distinct green color by the end of each experiment. Some cultures were sampled for observation under a microscope and did not show visual signs of bacterial contamination.

Comparing growth of *C. vulgaris* in the presence of ferrihydrite to hematite or $FeCl_2$, the positive control and the culture containing $FeCl_2$ showed highest final cell numbers (~$45x10^6$ cells mL^{-1} and ~$35x10^6$ cells mL^{-1}, respectively) and highest growth rates (0.386 day^{-1} and 0.363 day^{-1}, respectively). These growth rates are similar to previously measured growth rates during *C. vulgaris* incubation [28],[6] (between 0.3 and 0.4 day^{-1}). Analysis of variance (ANOVA) indicated significant variation between the growth of different cultures ($p = 2.5x10^{-8}$). A post hoc Tukey's test on individual pairs showed there is a significant variation between all pairs, except for comparing growth between the negative control culture and the culture that contained hematite. growth in the presence of ferrihydrite and growth in the presence of ammonium ferric citrate green, $FeCl_2$ or hematite, as well as between the positive and negative controls.

The second-best growth rate has been measured in the culture containing $FeCl_2$ despite the concentration of $FeCl_2$ being three orders of magnitude lower than the concentration of the other types of iron and the absence of organic agents in cultures containing $FeCl_2$.

This observation coincides with our expectations and can be explained by both ammonium ferric citrate green (iron component in the positive control) and $FeCl_2$ being highly soluble salts[43,44], which dissociate almost completely and very quickly. Both ferrihydrite and hematite are mostly insoluble iron oxides, which makes them less bioavailable to microalgae, in comparison with the highly soluble iron salts mentioned above. Several processes need to happen in order for the microalgae to be able to adsorb the iron (and afterwards to absorb it), which are described in detail below. Qualitatively, this experiment showed that the concentration of dissolved ferric ions in the ferrihydrite and hematite solutions was most likely lower than 0.015 μM (since that was the concentration of $FeCl_2$).

Measurements of pH in the same experiment verified that on day 0, the pH values of all cultures ranged between 7 and 8. The pH of BG11 growth medium is set to be 7.1, therefore at culture start the low number of cells will drastically affect the pH. Part of the photosynthesis process is the uptake of dissolved CO_2 by the microalgae, which increases the pH of the surrounding solution[45]. It has also been shown that the uptake of H^+ by microalgae contributes to increase of the pH to more alkaline[45].

The growth of *C. vulgaris* cultures in the presence of ferrihydrite was compared between different types of organic ligands. All cultures contained ~$1x10^6$ cells mL^{-1} on day 0. Two cultures showed the most prominent growth – the one grown in the presence of ferrihydrite and LHA (final count of 13.72 ± 0.20 $x10^6$ cells mL^{-1} and a growth rate of 0.341 day^{-1}) and the culture that contained ferrihydrite without added organic agents (final count of 9.45 ± 6.36 $x10^6$ cells mL^{-1} and growth rate of 0.256 day^{-1}). ANOVA statistics performed on the cell measurement results revealed that there is a significant difference between the growth of these cultures ($p = 0.03$). A post hoc Tukey's test on individual pairs showed there was no significant variation between growth in the presence of LHA, compared to growth in the presence of citric acid and EDTA, compared to growth in the absence of organic agents. There was also no significant variation between the positive and negative controls. The only significant variation was found between the growth of the culture that contained ferrihydrite and LHA and the culture that contained the negative control ($Q_{0.05} = 4.748$, $Q_{calc} = 5.126$)

Q_{calc} or HSD (honestly significant difference) is a value calculated using Equation 4. Q_{crit} is the value for a specific confidence level α taken from a studentized range distribution table.

$$Q_{calc} = HSD = \frac{|M_i - M_j|}{SE} \qquad \text{(Equation 4)}$$

Where M_i and M_j are means of the compared pair and SE is the standard error of the sum of means.

The high growth rate of microalgae cells in the presence of ferrihydrite and LHA can be explained by the role of LHA, which serves as both an organic chelating agent for ferrihydrite and as an additional source of nutrients for the microalgae, including iron, as will be explained in detail below.

However, the high growth rate of the culture that contained ferrihydrite without organic agents contradicted our expectations, namely higher bioavailability in the presence of organic agents. We expected other cultures to grow faster, such as the culture that contained ferrihydrite and additionally CA and EDTA or the positive control, which contained a highly soluble source of iron in the same concentration as the ferrihydrite. Organic molecules are likely to increase the dissolution of iron as they weaken the bond between Fe and O. However, it has been shown that they can also inhibit it by adsorbing to the surface of the iron oxide particle and thus preventing protons or electrons from adsorbing[9].

It is unclear why an iron oxide without chelating agents promoted growth so well. It should also be mentioned that the SE of the set of triplicate data measuring the growth in the presence of ferrihydrite is quite large compared to the mean value. This describes a large variance between the results, the mean result therefore does not represent the individual measurements.

The slow growth of microalgae in the presence of ferrihydrite, CA and EDTA can be explained by the observation that under acidic pH a stable complex is formed between EDTA and iron atoms on the surface of the iron oxide particle, which might delay the uptake of iron. However, at basic pH (which was observed in our experiments) the stability of the complex is lower, facilitating the uptake[9]. The pH in our experiments obviously could not account for alleged lower bioavailability of ferrihydrite.

On day 0 the culture that contained ferrihydrite and LHA had a very high pH of 9.46, compared to the other cultures with pH values between 6.98 - 7.08. This can be explained by the presence of LHA in solution – the surface of LHA particles is covered with negatively charged functional groups such as carboxyl and phenolic OH. Upon addition to a solution, the negatively charged groups bind protons from the solution, thus increasing the solution's pH[46]. The culture with containing ferrihydrite and LHA showed a pH decrease on day 1 to 7.24, which can be explained by the humic acid releasing protons into the solution. The gradual increase in pH in all cultures starting from day 1 can be explained by the uptake of CO_2 and H^+ during photosynthesis as mentioned above.

Quantum yield measurements calculate the ratio between the variable fluorescence (F_V) and maximal fluorescence (F_M) of Photosystem II in dark-adapted photosynthetic samples. Light energy absorbed by chlorophyll molecules in photosynthetic organisms can undergo one of three fates: it can be used to drive photosynthesis (photochemistry), excess energy can be dissipated as heat, or it can be re-emitted as light (chlorophyll fluorescence). Quantum Yield of Photosystem II describes the ratio of fluorescence in dark adapted samples, when all photosystems are "open" and ready to work (Fv) and the maximal fluorescence (FM) in strong light, when all photosystems are "closed". In that case the light cannot be used in photochemistry, but instead is released as fluorescence. QY measurements of these cultures at day 0 gave values of 0.60 - 0.62 indicating lower efficiency of PSII at the beginning of the experiment (as mentioned in Section 2.5, QY values of 0.7 – 0.8 have been previously reported for healthy microalgae cultures). Low values mean the photosynthesis process being less efficient[47], algae cells in the lag phase are still adapting to the new environment and not performing efficient photosynthesis. Increased values are observed for all cultures on days 3 and 5, indicating that the cells have adapted and perform efficient photosynthesis, which in turn positively affects cell growth. The values remain in the range of 0.75-0.77 for all cultures except for the negative control, which points towards a less functional photosynthesis process. This

can be explained by the lack of iron in the negative control, as it is crucial to the photosynthesis process, for example as a component of iron-sulfur centers in PSI[48].

The third experimental setup was designed to test how LHA can affect growth of microalgae in the presence of different species of iron. The experiment began with similar cell counts in all cultures (~$1x10^6$ cells mL^{-1}). After 10 days there was a noticeable difference between the number of cells in cultures that contained LHA and cultures that didn't (in the presence of LHA contained cultures at day 10 more than ~6 $x10^6$ cells mL^{-1} while the positive and negative controls only contained 3.19 ± 0.80 $x10^6$ cells mL^{-1} and 1.41 ± 0.19 $x10^6$ cells mL^{-1}, respectively). ANOVA revealed the difference to be significant ($p = 2.64 \times 10^{-7}$). A post hoc Tukey's test on individual pairs showed significant variation between the pairs mentioned in **Table A4.2**, (Q_{calc} is higher than Q_{crit}).

These results support our hypothesis that LHA adds extra nutrients to the culture. LHA belongs to the group of humic acids and binds different elements which sustain microalgal growth, such as iron, P and S[50]. In this way it has growth-promoting or inhibiting functions, depending on their concentrations[49]. Therefore, it is not surprising that all cultures containing LHA outperformed the negative control and that cultures containing ferrihydrite and LHA outperformed the positive control significantly. In comparison with positive control, it is difficult to assess the influence of ferrihydrite vs. LHA in enhancing growth. The exponential growth rate in the presence of 23 µM of ferrihydrite (0.251 day^{-1}) was lower than the growth rate in the presence of 0.15 nM of ferrihydrite (0.267 day^{-1}), however the difference in growth between the two cultures was not significant based on Tukey's test.

The pH in the cultures of this experiment at day 0 was higher in cultures that contained LHA (between pH 8.65 - 9.13) than in the positive or negative controls (pH 7.35 and 7.12, respectively). At day 1 the pH values decreased in all cultures containing LHA, but from this day onward steadily increased in all these cultures. This observation attributed to the higher growth rates as discussed before, photosynthesis increased the pH values in the solutions and higher cell numbers absorbed more CO_2 from the solution.

All cultures started with QY values around 0.6, but as the experiment progressed the QY values increased gradually. However, this increase was less prominent for the negative control (from 0.60 to 0.66), which supports its lower growth compared to cultures that were grown in the presence of iron (their QY values ranged between 0.75 - 0.77). The difference in QY values measured in the negative control and in the cultures grown in the presence of LHA, including the positive control, was significant. The difference in all other measurements was not significant between cultures grown in the presence of different types of iron to cultures with ferrihydrite. We therefore can conclude that the addition of LHA did not have a significant effect on the functionality of the photosynthetic complex in *C. vulgaris* cells.

When discussing the bioavailability of iron species and their effect on microalgal growth, we should address both the solubility of the iron species, which is affected by the pH of the solution, as well as the rate at which they dissolve. Each species has a unique K_{SP} (solubility product) affected by pH and the size of the particles. The solubility product also depends on presence of other ions in the solution, since the solubility will be reduced by ions of the same species and increased by ions of other species[9].

Ferrihydrite and hematite are ferric oxides, they therefore are characterized by low solubility[9]. The rate of their dissolution is affected, among other factors, by the surface area, which is a function of particle size. The log K_{SP} of ferrihydrite was previously calculated as 3.54[9] and for hematite it was calculated to be 0.09 (the lower the K_{SP} value, the less soluble the compound is). A low K_{SP} also indicates low bioavailability of iron for *C. vulgaris*. Some of the iron (depending on solubility mentioned above) in iron oxide particles can dissolve into aqueous solution as a result of protonation or reduction, or a combination of both. In the process of protonation, first a proton is adsorbed to the iron oxide particle. The adsorption weakens the bond between Fe and O until it breaks, Fe^{3+} is detached and can be taken up by microalgae. Adsorption and therefore surface area of the sorbate are important in the process. In the case of dissolution of iron as a result of reduction, an electron transfer to the iron oxide will result in reduction of ferric iron to ferrous iron. This leads to Fe^{2+} to be released into solution, available for uptake by microalgae. Reduction can also occur in microalgae as a result of ferrireductase activity on the surface of the cells or by photoreduction[51].

Growth experiments with *Pyramimonas* sp. and *G. theta* were not successful. The number of cells for the former decreased 10 times over the course of 10 days, while the number of cells in the latter was not counted on day 10 since the culture appeared to be dead. Both algal species are more sensitive and less robust than *C. vulgaris*. Instead of growing the *G. theta* culture directly at 4°C, the cells most likely first should have adapted to the cold temperature. It would have been better to ease the transfer from 20 to 4°C by lowering the temperature stepwise. *Pyramimonas* sp. is grown at 4°C in the NORCCA culture collection, so instead of temperature the transfer from Norway to our laboratory (the cells were in a box for about a week before they were transferred to fresh medium) did cause stress that prevented the culture from thriving.

4.3 Iron content in microalgae cultures and LHA

As described in Section 2.7, prior to ICP-OES analysis the samples were filtered and then acidified using HNO_3 to prevent precipitation of iron oxides. The order of those steps has been examined by comparing concentrations of iron in solutions that were first acidified and then filtered, as opposed to solutions that were first filtered and then acidified (results in **Table A2.1**). A t-test (significance $\alpha = 0.05$) showed there was no significant difference between the two methods.

The ICP-OES analysis was performed on samples taken at day 0 and day 5 of *C. vulgaris* cultures grown in the presence of iron and organic agents (Section 3.2, **Figure 3**). In most samples the iron concentrations were found to be below the detection limit. Only cultures growing on 0.15 nM of ferrihydrite or 23 µM hematite (at day 0) were calculated to contain 1.13 ± 0.11 µM and 1.18 ± 1.03 µM iron on day 5, respectively. The positive control triplicates were calculated to contain 19.53 ± 0.15 µM on day 0 and 0.07 ± 0.06 µM on day 5. However, the measurements performed on cultures grown in the presence of hematite showed large variations in the triplicate measurements. Due to the low number of measurements, it is not possible to exclude possible outliers, these results will therefore not be taken into consideration when discussing the iron content. As expected, the iron concentration in the negative control was below detection, no iron was added to these cultures.

Most noticeable was the difference in iron concentration between the positive control and the cultures containing LHA. It might be explained with the affinity of iron oxides[54] to humic acids such as LHA, which occurs very fast in the solution. A recent study has shown that in solution about 95% of iron is bound to humic acid within 24 hours[46]. Further it was suggested that the binding between humic substances and iron happens

immediately[55]. Alternatively, the iron might have been adsorbed rapidly to the outer walls of the microalgae cells. A high affinity between *C. vulgaris* and iron oxide nanoparticles has been reported previously[56]. By the time the samples were prepared for measurement, about 6 hours after the iron was added to the microalgae solutions, the iron was already adsorbed on the cell walls and thus undetectable by ICP-OES since microalgae cells cannot pass through 0.22 μm filter and thus are excluded from the filtered liquid.

As mentioned in Section 4.1, LHA is known to contain nutrients such as iron. We wanted to quantify the content of iron in our LHA standard and to explore whether this amount would be a significant addition to the iron provided to the microalgae. When preparing samples for ICP-OES, internal standards, such as yttrium or scandium[57] are used. In our experiments the intensity of argon gas served as an internal standard since it was present in the plasma in the same amount during sample analysis. Iron was extracted from LHA using two different concentrations of HCl, a control using MQ water for extraction was analyzed as well by ICP-OES. Each method of extraction resulted in a filtered solution that was diluted three times, for three different measurements. Since we did not know the concentration of iron in the samples at least one sample would fall within the limits of the calibration curve. Each dilution was measured using one biological replicate.

Unfortunately, the variation between the measurements was high. The results of 1 M HCl extraction showed the mean concentration of extracted iron to be 1.89 ± 0.40 mM. In the measurements using water or 12 M HCl for extraction the dilutions differed from each other by one order of magnitude but should be similar since we multiplied the resulting intensity by the dilution factor. This might be explained by a mistake made while diluting the original filtered solution by factors of 10, 100 and 1000. Alternatively, the calibration curve might be misleading. Both calibration curves (Section 3.1) have a very good linear relationship between the concertation of the standards and their measured intensity (R^2 = 0.9997 and R^2 = 0.99999). However, "perfect calibration curves" are usually measured over a wide range of concentrations. When fitting them into a linear plot, standards with higher concentration are taken more into account than the standards with the smallest concentration. This can have an impact on the accuracy of measurements of samples with lower concentration[58]. In this case however, the same effect should have been observed on the results using 1 M HCl for extraction.

Concerning the method chosen to extract iron from LHA, we need to consider the mechanism behind acid digestion or extraction of metals from organic samples. Metals such as iron tend to be part of the sample matrix in the form of insoluble iron oxides. Therefore, it is necessary to use an oxidizing agent to break the bonds between the iron and oxygen atoms and release the iron as ferrous or ferric ions into the solution. Such a release is visible as orange-red color in the solution (as seen in Section 3.2). HCl is considered to be a mild oxidizing agent, compared to others, such as HNO_3. Therefore, if an accurate quantification of total iron content in a sample is necessary, e.g. several steps using aqua regia (concentrated HNO_3 and HCl in a 3:1 ratio) combined with an additional heating step. The HNO_3 dissolves the organic matrix, while HCl releases the iron ions into the solution. However, using HCl has the advantage of adding Cl^- to the solution, which can form a complex with Fe and facilitate the release of iron into the solution[9].

To measure the iron content in LHA, an extraction was performed using only one strong acid at room temperature. We expected the iron concentration to be higher in both HCl extractions, compared to water. Since results from extractions using MQ water and 12 M HCl were inconclusive, as explained above, they were not used to draw conclusions

regarding iron content in LHA. If we consider only the extraction made with 1 M HCl, the total iron content of LHA is close to 2 mM, which translates to 0.111 g L^{-1} of iron in the LHA stock solution.

4.4 Characterization of ferrihydrite

XPS analysis was performed on two samples (Section 3.3). The first one contained ferrihydrite in a microalgae solution and was analyzed because we wanted to know whether it would be possible to detect ferrihydrite nanoparticles in an air-dried sample of one of our *C. vulgaris* cultures. We were also interested to see whether we can detect ferric or ferrous iron in the sample, since XPS allows for this kind of determination.

The resulting spectrum was analyzed by assigning peaks to specific elements and orbitals. No peaks relating to Fe were observed, probably due to a very low concentration of iron in the sample (the added amount on day 0 was 23 μM, the XPS sample was taken on day 5 of the experiment). As shown in Section 4.2, ICP-OES analysis of iron content in *C. vulgaris* culture after five days of incubation showed the sample contained 1.13 ± 0.11 μM, meaning there was a relatively small amount of iron in the solution to be detected. Carbon, oxygen and nitrogen as well as other expected elements were identified by their peaks. However, it was surprising to find peaks that suggest the presence of Si since no Si should be present in BG11 medium. This finding was supported by previously reported experiments during which XRD and XRF analysis done on leonardite revealed Si as a major element component[59].

A second sample that was analyzed by FTIR was the LHA standard. We wanted to check whether we can identify iron on the surface of LHA or close to it, since usually the surface sensitivity XPS is reported to be 10 nm[60]. Peaks that can be attributed to oxygen and carbon were seen (as expected since this is organic matter) but no peaks of Fe were identified. Therefore, it was decided to perform an extraction of iron from LHA, as described in Section 4.2.

FTIR analysis was performed on $FeCl_2$ and ferrihydrite stock solutions, prior to the beginning of growth experiments. When using ferrihydrite in experiments, one concern can be the transformation of the less thermodynamically stable ferrihydrite into the more stable hematite or goethite. This process can be delayed by the presence of phosphates, silicates and organic compounds[9]. FTIR analysis of the ferrihydrite stock solution has showed no peaks characteristic to hematite or goethite. In the case of $FeCl_2$ powder, it was suspected it had a lot of exposure to air, which can cause oxidation of ferrous iron into ferric iron. The analysis confirmed the powder contained only ferrous iron.

Samples from cultures containing ferrihydrite from one of the growth experiments were analyzed as well. Since those samples contained microalgae, it proved to be difficult to identify peaks related to ferrihydrite since those peaks are expected in a region where we also expect to see peaks caused by presence of microalgae. Since microalgae were present at a much higher concentration in the solution compared to ferrihydrite, the peaks resulting from their presence were more dominant in the spectra. As described in Section 3.3, samples from one of the growth experiments were submitted for FTIR analysis as well. Several peaks that are expected to be found when analyzing *C. vulgaris* were found on the spectra in ranges previously reported. An OH peak characteristic to iron oxides was expected to be found ~3600 cm^{-1}, however that area coincides with a wide peak that is attributed to water, which made it impossible to distinguish between the two.

Characterizing the ferrihydrite we worked with also included a discussion regarding the functional groups on its surface. This ties with the discussion above regarding the surface functional groups on LHA and microalgae since the question of adsorption between all three is at the core of this project. It has been previously shown that the surface groups of ferrihydrite include OH and COOH groups, which are pH sensitive (will be protonated at acidic pH). The majority of reaction sites consist of single coordinated -OH (O connected to one Fe atom) and double-coordinated μ-OH (an oxo group in which O is connected to two Fe atoms) groups[61]. The density of the singly coordinated sites was previously calculated to be 5.6 sites nm^{-2} or 6.4 sites nm^{-2}, depending on the structure of the nanoparticle[62]. Previous studies have also shown that ferrihydrite nanoparticles have a large surface area of about 600 $m^2 g^{-1}$ [63], which will promote adsorption, due to a large number of adsorption sites.

The next step was to calculate the theoretical concentration of said adsorption sites (as mentioned in Section 3.3), which resulted in 2.6 mM sites. It should be noted that in this calculation, a lower surface area value has been used (200 $m^2 g^{-1}$) since the higher values are usually reported for freshly prepared ferrihydrite[64] whereas our stock can be considered more aged as it was prepared about a year ago.

The calculated concentration of binding sites on the surface of ferrihydrite (2.6 mM) was compared to the concentration of phosphate in our culture flasks (0.23 mM). Since the former is one order of magnitude above the latter, we can assume that even in the case of all phosphate anions were quickly adsorbed to the ferrihydrite surface, most of the phosphate remained dissolved in the medium and was available to support growth of microalgae, as we saw empirically in the experiments in this project.

We wanted to determine the surface charge of ferrihydrite particles since it is directly correlated to their aggregation and their adsorption to microalgae. As has been mentioned above, adsorption is the first step in a process of uptake by microalgae cells which have a negative surface charge under biological pH conditions. The particle size plays a role in uptake as well, since larger particles will have a slower diffusion rate and thus be less bioavailable than relatively smaller particles. We know based on our measurements using Multisizer (which in addition to cell count, also provides a report regarding the size distribution of cells) that the size of *C. vulgaris* in our flasks was about 4-6 μm.

Zeta potential values were measured across a range of pH (6.0 - 9.0) to find the point of zero charge (PZC). This is an important attribute of every particle in a solution since it describes the surface charge of the particle, and more accurately the electrical potential at the furthest point of the electrical double layer from the solid surface of the particle[65] (the “slipping plane”). We wanted to find it for ferrihydrite to understand under what pH range it is more likely to aggregate since aggregation of iron oxide particles can limit their bioavailability. In other words, we wanted to see how the stability of the colloidal ferrihydrite solution changes as a function of pH.

This PZC can be empirically found by exposing the particles in the solution to a range of pH we are interested in (essentially, preforming a titration) and measure the zeta potential at fixed intervals. The measured zeta potential value fluctuated as a function of pH, as expected. In the case on a negatively charged particle with a negative value of zeta potential, acidic pH means there are more protons in the solution which will cause the particles to be surrounded by positively charged ions until the negatively charged functional groups will be protonated and eventually neutral. This will reduce the thickness of the electric double layer and the zeta potential will decrease as well (until

reaching the PZC). Alkaline pH will increase the concentration of anions in the solution, which will cause deprotonation of the functional groups and their increasing negativity (correlated with increasing negative zeta potential) will cause the particles to repel each other.

Another factor to consider when discussing surface charge is that high ionic strength will be correlated with lower zeta potential, lower surface charge and higher tendency to aggregate. This is according to the DLVO theory which describes the stability of colloidal suspensions as being affected by two factors – the repulsion between particles due to electrostatic interactions and attraction between particles due to Van der Waals forces[34].

The empirical point of zero charge was found to be to be at pH 8.9, as expected based on previous reported values[66]. This means that at this pH the particles are expected to aggregate. At lower pH ranges the particles are expected to be positively charged, as can be seen in Section 3.3, where Zeta potential ~20 mV was measured in a solution with pH 5.5. This measurement provided us with an assessment that in the range of pH of our microalgae growth experiments, the surface charge of ferrihydrite is expected to be positively charged, with a growing tendency to aggregate as the experiments approach the last days during which the measured pH was around 9. It is important to remember that the zeta potential is affected by ionic strength, which in the case of BG11 is around 20 mM at pH of around 7.

Particle size of ferrihydrite was measured over a range of pH 5.5 - 9. In this measurement, we wanted to see what is the extent of aggregation that actually happens in the solution as the pH increases. It is important to remember that the results reflect the hydrodynamic diameter of the particles, which is the size of the particle in an aqueous solution (and not when it is in the form of dry powder, for example).

The results of those measurements were not conclusive since the at pH 7 - 7.5 the particles were measured at a wide range of sizes, from about 7 to 35 μm. This goes against expectations that at a certain pH the size measurements will be less dispersed (such as in the case of pH 5.5). It is not just the large variation of size at pH 7 which is unexpected. The measured hydrodynamic diameter, its lowest value being 1.85 μm, is three to four orders of magnitude above what we expect to see in ferrihydrite nanoparticles which have previously been reported to measure 2 - 3 nm when freshly prepared and can also reach 7 – 8 nm[63]. In the case of such large particles as measured in our experiment, microalgae are very unlikely to be able to adsorb the ferrihydrite particles since microalgae cells themselves measure a few microns in diameter. However, we see in the growth measurement experiments that growth occurs in the presence of ferrihydrite as the only source of iron, meaning these results probably do not reflect the true size of the nanoparticles in our cultures.

In addition to the above, a measurement of hydrodynamic diameter of ferrihydrite was done in a concentrated solution of ferrihydrite at pH 6, which resulted in a mean value of 158 nm. This is still two orders of magnitude higher than expected. A separate measurement of zeta potential of *C. vulgaris* cells in BG11 culture at pH 7.1 resulted in electric potential of -28 mV, which empirically proves that our microalgae cells are negatively charged. This value coincides with other reported measurements[67].

It should be taken into consideration that the ionic strength of the ferrihydrite solution (6.72 mM at pH of ~7) was different than in the flasks, which can affect the stability of

the nanoparticles. It has been previously calculated that the ionic strength of BG11 is 23.44 ± 0.30[68] mM when it is prepared at approximately 7.1 pH.

5. Conclusions and Outlook

The aim of this project was to investigate the bioavailability of ferrihydrite nanoparticles to microalgae, specifically *C. vulgaris* and two other cold-adapted species, compared to other forms of iron in the presence and absence of organic chelating agents. Several experiments were planned in order to provide reliable data to achieve this aim and to understand the microbiology and inorganic chemistry behind it. Our hypothesis stated that when it comes to bioavailability, the less thermodynamically stable ferrihydrite will have a clear advantage over the stable and less soluble hematite. It also defined our goal to explore the uptake of iron not just by *C. vulgaris*, but also by species that were adapted to cold conditions. Unfortunately, preliminary experiments using the cold-adapted *Pyramimonas* sp. and *G. theta* were not successful and did not contribute to conclusions regarding our hypothesis.

The results of our experiments support our hypothesis by showing ferrihydrite indeed being more bioavailable than hematite. Growth rates of microalgae cultures in the presence of different types of iron decreased in the following order – positive control > culture with $FeCl_2$ > culture with ferrihydrite > negative control > culture with hematite. These growth rates suggest that ferrihydrite was indeed significantly more bioavailable than hematite, as a result of ferrihydrite's higher solubility, compared to hematite. When comparing solutions that contained ferrihydrite and different organic agents, no significant differences were found between the growth rates, meaning that we cannot draw conclusions regarding how different organic agents affect ferrihydrite's bioavailability.

Based on calculated growth rates, it can be concluded that the addition of LHA is indeed a factor that dramatically improves growth. This can be attributed to LHA's nutrient content, specifically iron (as was measured in this project using ICP-OES). The only significant difference in growth when comparing cultures that contained added iron, was found between the positive control and the culture that contained ferrihydrite and LHA. Unfortunately, there was no further insight regarding the role of ferrihydrite or LHA in solutions that include both, since it is not clear how much each component contributed to promoting the growth of the cells.

Results of ICP-OES measurements of iron concentration in solutions containing microalgae and LHA have highlighted the rapid binding of iron, either to microalgae cells or LHA, which seemingly occurred within several hours. It can be beneficial to further explore the relationship between humic acids, iron oxides and microalgae perhaps to combine the metal removing abilities of both microalgae and humic acids for a more effective process of cleaning wastewater.

Measurements of electrical potential on the surface of ferrihydrite particles has showed that in pH range of 7-9 ferrihydrite particles were positively charged, while microalgae cells have a negative surface charge. This further contributes to conclusion that adsorption was driven by electrostatic attraction forces and that it is pH-dependent.

Several aspects still remain unclear, such as whether we can attribute LHA's growth promoting abilities to the additional iron content it provided to the microalgae or to other nutrients present in humic acids. Another aspect that was not covered in this project relates to the implications of iron bioavailability when it comes to cold-adapted species

of microalgae. Additional research in this area can contribute to our understanding of iron uptake by microalgae in the Arctic and how it can be affected by environmental changes, such as climate change and polar ocean acidification.

In a broader context, as mentioned in the introduction, this project is a very small part of an enormous global group effort by hundreds of scientific lab groups to reach a better understanding how to create the optimal conditions for microalgae to thrive. The results here can serve as another point of data that might help future research groups, since some of the results have a direct connection to practical applications of the affinity between microalgae and metals (such as remediation of polluted water sources).

Acknowledgement

First of all, I would like to thank Christiane Funk and Jean-Francois Boily for the all the guidance and support they have provided me throughout this year. To Martin Plöhn – a huge thank you for your patience and the amount of time and energy you spent explaining basic (and not-so basic) concepts and showing me the ropes.

I would like to thank Andrey Shchukarev for performing the XPS measurements and helping me decipher them. A special thanks goes to Tao Chen for his kindness and willingness to help me with all the measurements that were done using the Zetasizer.

I would also like to thank all the members of the Funk and Schroeder labs on whom I relied so much for mental support (and the occasional scientific question), I don't think I would have managed without our silly lunch breaks and fikas. Luisa, Yolanda, Jack and Andre – you are the absolute best.

And finally, to my amazing mom and dad, and to my awesome sister. You have encouraged me to pursue this degree and supported me in every possible way, this would not be possible if it weren't for you. I am truly blessed to have you in my life.

References

1. Sustainable Development Goals | United Nations Development Programme. UNDP. [accessed 2023 Dec 19]. https://www.undp.org/sustainable-development-goals

2. Prasad R, Gupta SK, Shabnam N, Oliveira CYB, Nema AK, Ansari FA, Bux F. Role of Microalgae in Global CO2 Sequestration: Physiological Mechanism, Recent Development, Challenges, and Future Prospective. Sustainability. 2021;13(23):13061. doi:10.3390/su132313061

3. Zingone A, Oksfeldt Enevoldsen H. The diversity of harmful algal blooms: a challenge for science and management. Ocean & Coastal Management. 2000;43(8):725–748. doi:10.1016/S0964-5691(00)00056-9

4. Spain O, Plöhn M, Funk C. The cell wall of green microalgae and its role in heavy metal removal. Physiologia Plantarum. 2021;173(2):526–535. doi:10.1111/ppl.13405

5. Khan MI, Shin JH, Kim JD. The promising future of microalgae: current status, challenges, and optimization of a sustainable and renewable industry for biofuels, feed, and other products. Microbial Cell Factories. 2018;17(1):36. doi:10.1186/s12934-018-0879-x

6. Blair MF, Kokabian B, Gude VG. Light and growth medium effect on Chlorella vulgaris biomass production. Journal of Environmental Chemical Engineering. 2014;2(1):665–674. doi:10.1016/j.jece.2013.11.005

7. Sunda W, Price N, Morel F. Trace Metal Ion Buffers and Their Use in Culture Studies. Algal Culturing Techniques. 2005 Jan 1. doi:10.1016/B978-012088426-1/50005-6

8. Devadasu E, Subramanyam R. Enhanced Lipid Production in Chlamydomonas reinhardtii Caused by Severe Iron Deficiency. Frontiers in Plant Science. 2021 [accessed 2023 Dec 12];12. https://www.frontiersin.org/articles/10.3389/fpls.2021.615577

9. Schwertmann U. Solubility and dissolution of iron oxides. Plant and soil. 1991;130:1–25.

10. Rana MS, Prajapati SK. Resolving the dilemma of iron bioavailability to microalgae for commercial sustenance. Algal Research. 2021;59:102458. doi:10.1016/j.algal.2021.102458

11. Liu X, Millero FJ. The solubility of iron in seawater. Marine Chemistry. 2002;77(1):43–54. doi:10.1016/S0304-4203(01)00074-3

12. Raiswell R, Canfield D. The Iron Biogeochemical Cycle Past and Present. Geochemical Perspectives. 2012;1:1–220. doi:10.7185/geochempersp.1.1

13. de Melo BAG, Motta FL, Santana MHA. Humic acids: Structural properties and multiple functionalities for novel technological developments. Materials Science and Engineering: C. 2016;62:967–974. doi:10.1016/j.msec.2015.12.001

14. Stanier RY, Kunisawa R, Mandel M, Cohen-Bazire G. Purification and properties of unicellular blue-green algae (order Chroococcales). Bacteriological Reviews. 1971;35(2):171–205. doi:10.1128/br.35.2.171-205.1971

15. Ru ITK, Sung YY, Jusoh M, Wahid MEA, Nagappan T. Chlorella vulgaris: a perspective on its potential for combining high biomass with high value bioproducts. Applied Phycology. 2020;1(1):2–11. doi:10.1080/26388081.2020.1715256

16. The Norwegian Culture Collection of Algae | NORCCA. [accessed 2023 Dec 6]. https://norcca.scrol.net/

17. Mendes CRB, Tavano VM, Dotto TS, Kerr R, de Souza MS, Garcia CAE, Secchi ER. New insights on the dominance of cryptophytes in Antarctic coastal waters: A case study in Gerlache Strait. Deep Sea Research Part II: Topical Studies in Oceanography. 2018;149:161–170. (Oceanographic processes and biological responses around Northern Antarctic Peninsula: a 15-year contribution of the Brazilian High Latitude Oceanography Group). doi:10.1016/j.dsr2.2017.02.010

18. WoRMS - World Register of Marine Species - Chlorella vulgaris Beyerinck [Beijerinck], 1890. [accessed 2023 Nov 28]. https://www.marinespecies.org/aphia.php?p=taxdetails&id=532029

19. UIO 569 | NORCCA. [accessed 2023 Nov 28]. https://norcca.scrol.net/strain/uio-569

20. WoRMS - World Register of Marine Species - Guillardia theta D.R.A.Hill & R.Wetherbee, 1990. [accessed 2023 Oct 25]. https://www.marinespecies.org/aphia.php?p=taxdetails&id=590566

21. Khalili A, Najafpour GD, Amini G, Samkhaniyani F. Influence of nutrients and LED light intensities on biomass production of microalgae Chlorella vulgaris. Biotechnology and Bioprocess Engineering. 2015;20(2):284–290. doi:10.1007/s12257-013-0845-8

22. Guillard RRL. Culture of Phytoplankton for Feeding Marine Invertebrates. In: Smith WL, Chanley MH, editors. Culture of Marine Invertebrate Animals: Proceedings — 1st Conference on Culture of Marine Invertebrate Animals Greenport. Boston, MA: Springer US; 1975. p. 29–60. https://doi.org/10.1007/978-1-4615-8714-9_3. doi:10.1007/978-1-4615-8714-9_3

23. Cheng W, Hanna K, Boily J-F. Water Vapor Binding on Organic Matter-Coated Minerals. Environmental Science & Technology. 2019;53(3):1252–1257. doi:10.1021/acs.est.8b05134

24. Morris R. Spectrophotometry. Current Protocols Essential Laboratory Techniques. 2015 [accessed 2023 Dec 7];11(1). https://currentprotocols.onlinelibrary.wiley.com/doi/10.1002/9780470089941.et0201s11. doi:10.1002/9780470089941.et0201s11

25. SECTION 1 - INTRODUCTION.pdf. [accessed 2023 Nov 30]. https://www.med.cam.ac.uk/wp-content/uploads/2014/10/coulter_manual.pdf

26. Masojídek J, Torzillo G, Koblížek M. Photosynthesis in Microalgae. In: Handbook of Microalgal Culture. John Wiley & Sons, Ltd; 2013. p. 21–36. https://onlinelibrary.wiley.com/doi/abs/10.1002/9781118567166.ch2. doi:10.1002/9781118567166.ch2

27. Iluz D, Dubinsky Z, Iluz D, Dubinsky Z. Quantum Yields in Aquatic Photosynthesis. In: Photosynthesis. IntechOpen; 2013. https://www.intechopen.com/chapters/45159. doi:10.5772/56539

28. Metsoviti MN, Papapolymerou G, Karapanagiotidis IT, Katsoulas N. Effect of Light Intensity and Quality on Growth Rate and Composition of Chlorella vulgaris. Plants. 2020;9(1):31. doi:10.3390/plants9010031

29. Gojkovic Ž, Vílchez C, Torronteras R, Vigara J, Gómez-Jacinto V, Janzer N, Gómez-Ariza J-L, Márová I, Garbayo I. Effect of Selenate on Viability and Selenomethionine Accumulation of *Chlorella sorokiniana* Grown in Batch Culture. The Scientific World Journal. 2014;2014:e401265. doi:10.1155/2014/401265

30. Ferro L, Gorzsás A, Gentili FG, Funk C. Subarctic microalgal strains treat wastewater and produce biomass at low temperature and short photoperiod. Algal Research. 2018;35:160–167. doi:10.1016/j.algal.2018.08.031

31. Inductively Coupled Plasma Optical Emission Spectroscopy (ICP-OES) Information - SE. [accessed 2023 Nov 6].

https://www.thermofisher.com/uk/en/home/industrial/spectroscopy-elemental-isotope-analysis/spectroscopy-elemental-isotope-analysis-learning-center/trace-elemental-analysis-tea-information/icp-oes-information.html

32. Costo R, Heinke D, Grüttner C, Westphal F, Morales MP, Veintemillas-Verdaguer S, Gehrke N. Improving the reliability of the iron concentration quantification for iron oxide nanoparticle suspensions: a two-institutions study. Analytical and Bioanalytical Chemistry. 2019;411(9):1895–1903. doi:10.1007/s00216-018-1463-2

33. Shahbazi K, Beheshti M. Comparison of three methods for measuring heavy metals in calcareous soils of Iran. SN Applied Sciences. 2019;1(12):1541. doi:10.1007/s42452-019-1578-x

34. Bhattacharjee S. DLS and zeta potential – What they are and what they are not? Journal of Controlled Release. 2016;235:337–351. doi:10.1016/j.jconrel.2016.06.017

35. Brinza L. Surface Coverage Simulation and 3D Plotting of Main Process Parameters for Molybdenum and Vanadium Adsorption onto Ferrihydrite. Nanomaterials. 2022;12(3):304. doi:10.3390/nano12030304
36. Heide P van der. X-ray Photoelectron Spectroscopy: An introduction to Principles and Practices. John Wiley & Sons; 2011.

37. Cleaning Laboratory Glassware. [accessed 2023 Oct 25]. https://www.sigmaaldrich.com/SE/en/technical-documents/protocol/chemistry-and-synthesis/reaction-design-and-optimization/cleaning-glassware

38. Moulder JF. Handbook of X-ray Photoelectron Spectroscopy: A Reference Book of Standard Spectra for Identification and Interpretation of XPS Data. Physical Electronics Division, Perkin-Elmer Corporation; 1992.

39. Duygu DY, Udoh AU, Ozer TB, Akbulut A, Erkaya IA, Yildiz K, Guler D. Fourier transform infrared (FTIR) spectroscopy for identification of Chlorella vulgaris Beijerinck 1890 and Scenedesmus obliquus (Turpin) Kützing 1833. African Journal of Biotechnology. 2012;11(16):3817–3824. doi:10.5897/AJB11.1863

40. Boily J-F, Szanyi J, Felmy AR. A combined FTIR and TPD study on the bulk and surface dehydroxylation and decarbonation of synthetic goethite. Geochimica et Cosmochimica Acta. 2006;70(14):3613–3624. doi:10.1016/j.gca.2006.05.013

41. Mendez JC, Hiemstra T. Surface area of ferrihydrite consistently related to primary surface charge, ion pair formation, and specific ion adsorption. Chemical Geology. 2020;532:119304. doi:10.1016/j.chemgeo.2019.119304

42. Sajjadi B, Chen W-Y, Raman AbdulAzizA, Ibrahim S. Microalgae lipid and biomass for biofuel production: A comprehensive review on lipid enhancement strategies and their effects on fatty acid composition. Renewable and Sustainable Energy Reviews. 2018;97:200–232. doi:10.1016/j.rser.2018.07.050

43. PubChem. Iron(III) ammonium citrate. [accessed 2023 Dec 10]. https://pubchem.ncbi.nlm.nih.gov/compound/91758680

44. PubChem. Ferrous Chloride. [accessed 2023 Dec 10]. https://pubchem.ncbi.nlm.nih.gov/compound/24458

45. Zerveas S, Mente MS, Tsakiri D, Kotzabasis K. Microalgal photosynthesis induces alkalization of aquatic environment as a result of H+ uptake independently from CO2 concentration – New perspectives for environmental applications. Journal of Environmental Management. 2021;289:112546. doi:10.1016/j.jenvman.2021.112546

46. Kiswanto K, Wintah W. Ability of Humic Acid in the Absorption of Heavy Metal Content of Lead and Iron in Fish Culture Media. Journal of Ecological Engineering. 2023;24(5):95–102. doi:10.12911/22998993/161328

47. Deamici KM, Cuellar-Bermudez SP, Muylaert K, Santos LO, Costa JAV. Quantum yield alterations due to the static magnetic fields action on Arthrospira platensis SAG 21.99: Evaluation of photosystem activity. Bioresource Technology. 2019;292:121945. doi:10.1016/j.biortech.2019.121945

48. Dao LHT, Beardall J. Effects of lead on two green microalgae Chlorella and Scenedesmus: photosystem II activity and heterogeneity. Algal Research. 2016;16:150–159. doi:10.1016/j.algal.2016.03.006

49. Popa DG, Lupu C, Constantinescu-Aruxandei D, Oancea F. Humic Substances as Microalgal Biostimulants—Implications for Microalgal Biotechnology. Marine Drugs. 2022;20(5):327. doi:10.3390/md20050327
50. Elemental Compositions and Stable Isotopic Ratios of IHSS Samples | IHSS. [accessed 2023 Nov 21]. https://humic-substances.org/elemental-compositions-and-stable-isotopic-ratios-of-ihss-samples/

51. Sutak R, Botebol H, Blaiseau P-L, Léger T, Bouget F-Y, Camadro J-M, Lesuisse E. A Comparative Study of Iron Uptake Mechanisms in Marine Microalgae: Iron Binding at the Cell Surface Is a Critical Step1[W][OA]. Plant Physiology. 2012;160(4):2271–2284. doi:10.1104/pp.112.204156

52. Tang C-C, Zhang X-Y, Wang R, Wang T-Y, He Z-W, Wang XC. Calcium ions-effect on performance, growth and extracellular nature of microalgal-bacterial symbiosis system treating wastewater. Environmental Research. 2022;207:112228. doi:10.1016/j.envres.2021.112228

53. Pirt SJ, Walach M. Biomass yields of Chlorella from iron (Yx/Fe) in iron-limited batch cultures. Archives of Microbiology. 1978;116(3):293–296. doi:10.1007/BF00417854

54. Yang R, Su H, Qu S, Wang X. Capacity of humic substances to complex with iron at different salinities in the Yangtze River estuary and East China Sea. Scientific Reports. 2017;7(1):1381. doi:10.1038/s41598-017-01533-6

55. Fang K, Yuan D, Zhang L, Feng L, Chen Y, Wang Y. Effect of environmental factors on the complexation of iron and humic acid. Journal of Environmental Sciences. 2015;27:188–196. doi:10.1016/j.jes.2014.06.039

56. Fraga-García P, Kubbutat P, Brammen M, Schwaminger S, Berensmeier S. Bare Iron Oxide Nanoparticles for Magnetic Harvesting of Microalgae: From Interaction Behavior to Process Realization. Nanomaterials. 2018;8(5):292. doi:10.3390/nano8050292

57. ICP-OES Data Analysis - SE. [accessed 2023 Dec 11]. https://www.thermofisher.com/uk/en/home/industrial/spectroscopy-elemental-isotope-analysis/spectroscopy-elemental-isotope-analysis-learning-center/trace-elemental-analysis-tea-information/icp-oes-information/icp-oes-data-analysis.html

58. whp_atomic_spectroscopy-effects_on_accuracy_and_detection_limits_013559_01.pdf. [accessed 2023 Dec 11]. https://resources.perkinelmer.com/lab-solutions/resources/docs/whp_atomic_spectroscopy-effects_on_accuracy_and_detection_limits_013559_01.pdf

59. Ratanaprommanee C, Chinachanta K, Chaiwan F, Shutsrirung A. Chemical characterization of leonardite and its potential use as soil conditioner and plant growth enhancement.

60. Stevie FA, Donley CL. Introduction to x-ray photoelectron spectroscopy. Journal of Vacuum Science & Technology A: Vacuum, Surfaces, and Films. 2020;38(6):063204. doi:10.1116/6.0000412

61. Boily J-F, Song X. Direct identification of reaction sites on ferrihydrite. Communications Chemistry. 2020;3(1):1–8. doi:10.1038/s42004-020-0325-y

62. Hiemstra T, Van Riemsdijk WH. A surface structural model for ferrihydrite I: Sites related to primary charge, molar mass, and mass density. Geochimica et Cosmochimica Acta. 2009;73(15):4423–4436. doi:10.1016/j.gca.2009.04.032

63. Hiemstra T. Surface and mineral structure of ferrihydrite. Geochimica et Cosmochimica Acta. 2013;105:316–325. doi:10.1016/j.gca.2012.12.002

64. Hiemstra T, C. Mendez J, Li J. Evolution of the reactive surface area of ferrihydrite: time, pH, and temperature dependency of growth by Ostwald ripening. Environmental Science: Nano. 2019;6(3):820–833. doi:10.1039/C8EN01198B

65. Overview_DLVO_Theory1.pdf. [accessed 2023 Dec 5]. https://colloid.ch/grouppage/pdf/Overview_DLVO_Theory1.pdf

66. Mendez JC, Hiemstra T. Surface area of ferrihydrite consistently related to primary surface charge, ion pair formation, and specific ion adsorption. Chemical Geology. 2020;532:119304. doi:10.1016/j.chemgeo.2019.119304

67. Matho C, Schwarzenberger K, Eckert K, Keshavarzi B, Walther T, Steingroewer J, Krujatz F. Bio-compatible flotation of Chlorella vulgaris: Study of zeta potential and flotation efficiency. Algal Research. 2019;44:101705. doi:10.1016/j.algal.2019.101705

68. Wang Z, Luo Z, Yan Y. Dispersion and sedimentation of titanium dioxide nanoparticles in freshwater algae and daphnia aquatic culture media in the presence of arsenate. Journal of Experimental Nanoscience. 2018;13(1):119–129. doi:10.1080/17458080.2018.1449023

Appendix

Appendix 1

Figure A1.1 Appearance of a ring of aggregated cells on one of the flasks during an experiment.

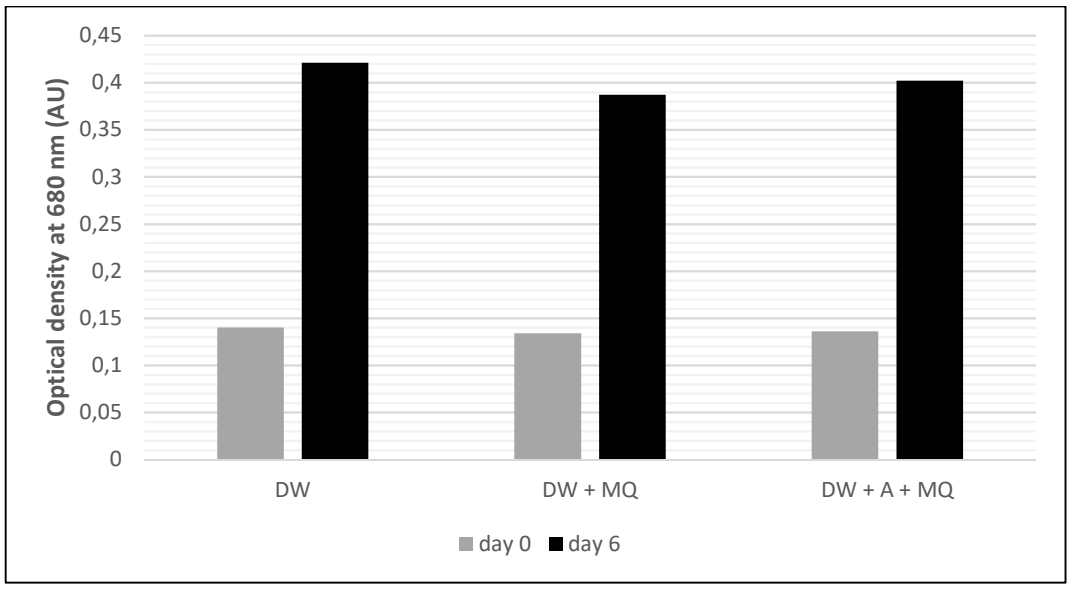

Figure A1.2 Algal growth (OD_{680}) of *C. vulgaris* in flasks that were washed using different methods (DW = dishwasher, MQ = MilliQ water, A = acid)

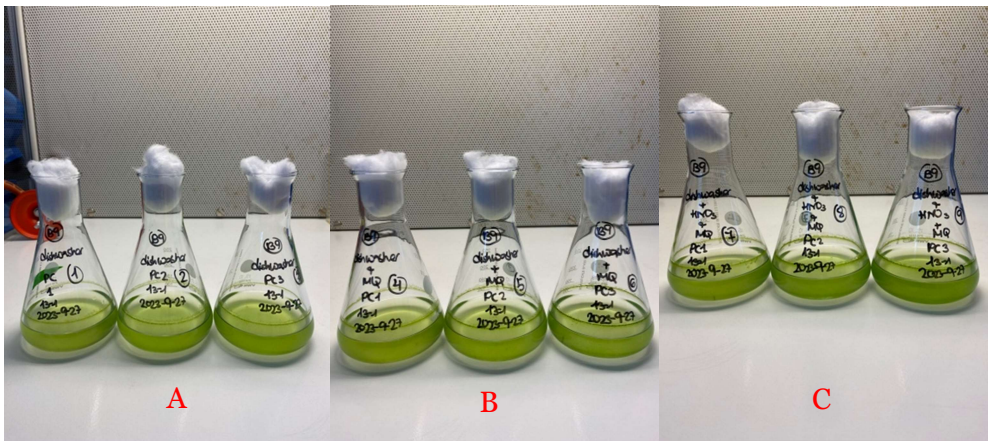

Figure A1.3 Appearance of aggregation on flasks that were washed using a dishwasher only (A), dishwasher followed by MQ (B), or dishwasher followed by acid bath and MQ (C).

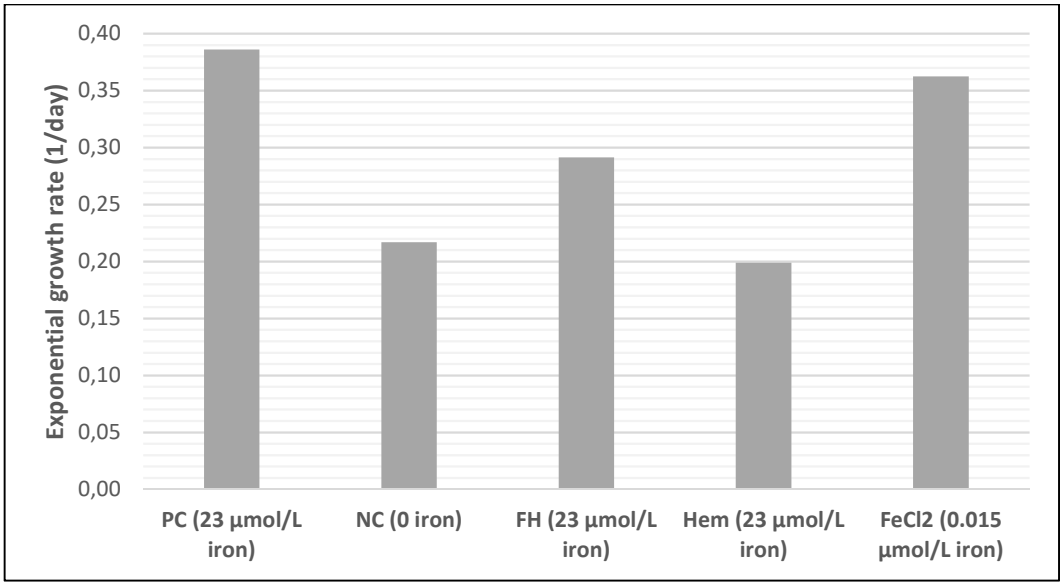

Figure A1.4. Exponential growth rates of *C. vulgaris* in the presence of different iron species. Positive control (PC, 23 µM ammonium ferric citrate green + $3.12x10^{-6}$ M CA + $3.4x10^{-7}$ M EDTA), negative control (NC, iron-depleted), ferrihydrite (FH 23 µM), $FeCl_2$ (0.015 µM) and hematite (Hem, 23 µM).

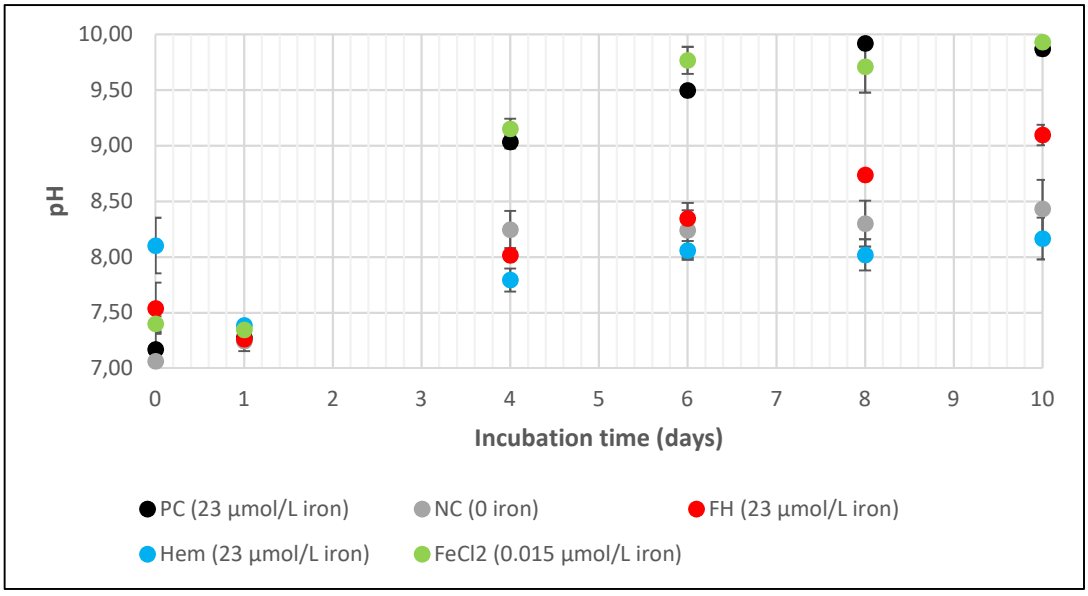

Figure A1.5 pH values of *C. vulgaris* cultures grown in the presence or absence of various iron species. Positive control (PC, 23 µM ammonium ferric citrate green + $3.12x10^{-6}$ M CA + $3.4x10^{-7}$ M EDTA), negative control (NC, iron-depleted), ferrihydrite (FH 23 µM), $FeCl_2$ (0.015 µM) and hematite (Hem, 23 µM)

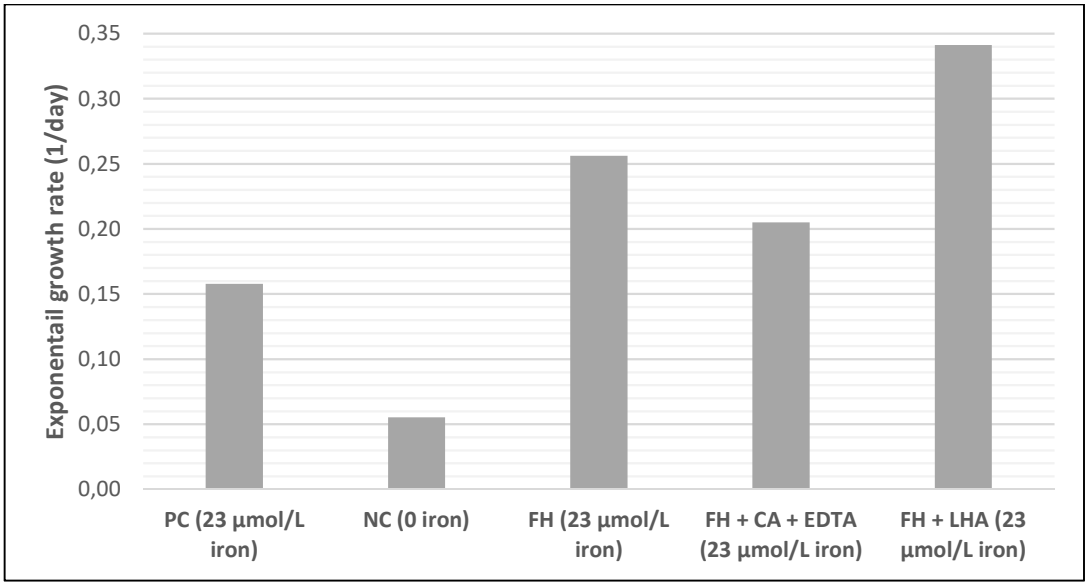

Figure A1.6. Exponential growth rates of *C. vulgaris* in the presence of iron and organic agents. Positive control (PC, 23 µM ammonium ferric citrate green + $3.12x10^{-6}$ M CA + $3.4x10^{-7}$ M EDTA), negative control (NC, iron-depleted + $3.12x10^{-6}$ M CA + $3.4x10^{-7}$ M EDTA), ferrihydrite in the absence of organic agents (FH, 23 µM), ferrihydrite in the presence of citric acid and EDTA (FH 23 µM + $3.12x10^{-6}$ M CA + $3.4x10^{-7}$ M EDTA) and ferrihydrite in the presence of LHA (FH 23 µM + 5% LHA).

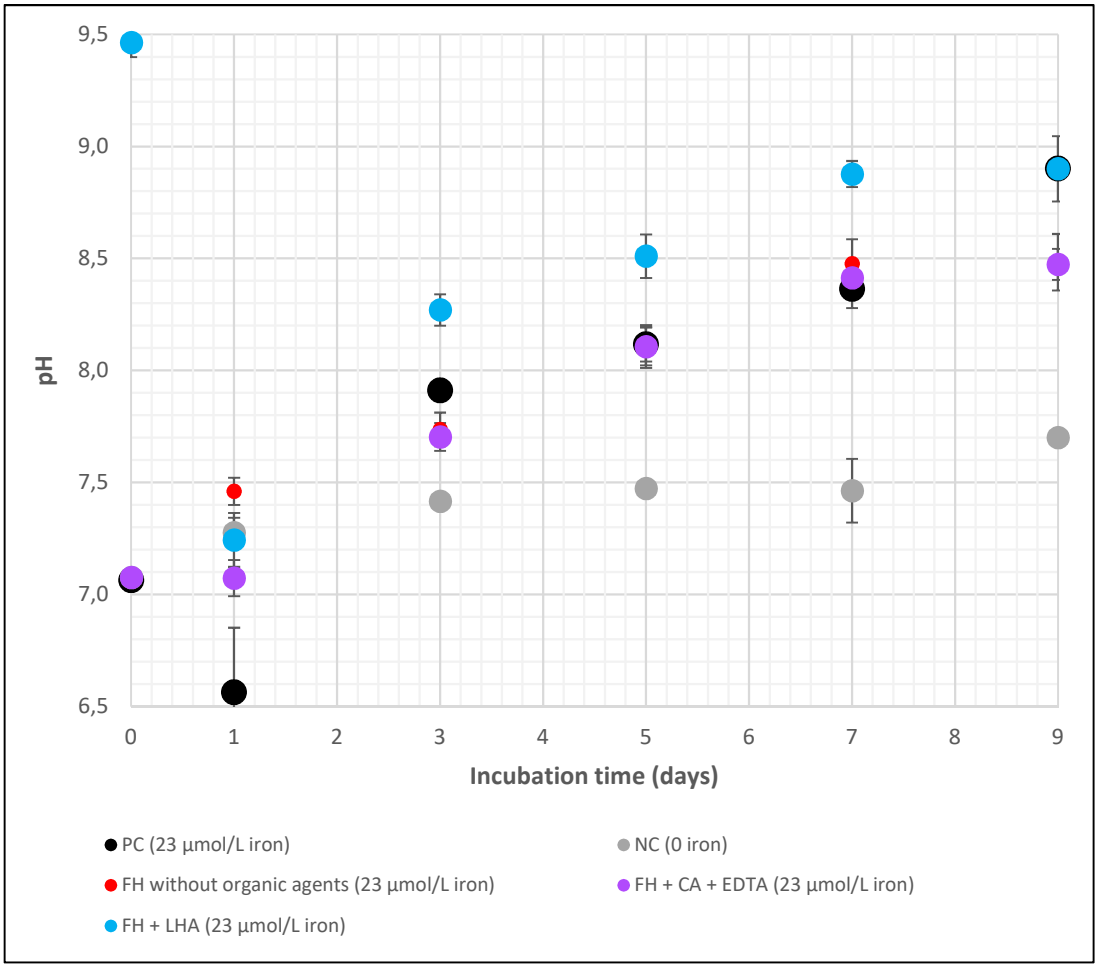

Figure A1.7 pH values of *C. vulgaris* cultures in the presence or absence of ferrihydrite and varying components of organic agents. Positive control (PC, 23 µM ammonium ferric citrate green + $3.12x10^{-6}$ M CA + $3.4x10^{-7}$ M EDTA), negative control (NC, iron-depleted + $3.12x10^{-6}$ M CA + $3.4x10^{-7}$ M EDTA), ferrihydrite in the absence of organic

agents (FH, 23 µM), ferrihydrite in the presence of citric acid and EDTA (FH 23 µM + $3.12x10^{-6}$ M CA + $3.4x10^{-7}$ M EDTA), ferrihydrite in the presence of LHA (FH 23 µM + 5% LHA). Mean values □ SE (n = 3) are presented

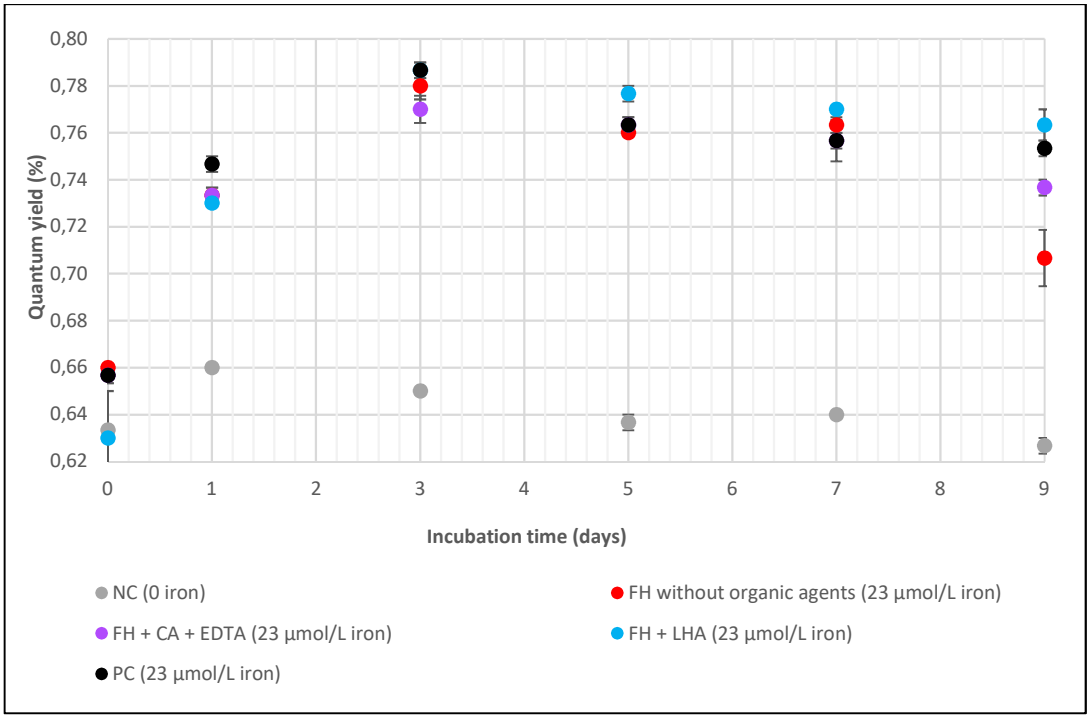

Figure A1.8 Quantum yield of *C. vulgaris* in the presence or absence of ferrihydrite and varying components of organic agents. Positive control (PC, 23 µM ammonium ferric citrate green + $3.12x10^{-6}$ M CA + $3.4x10^{-7}$ M EDTA), negative control (NC, iron-depleted + $3.12x10^{-6}$ M CA + $3.4x10^{-7}$ M EDTA), ferrihydrite in the absence of organic agents (FH, 23 µM), ferrihydrite in the presence of citric acid and EDTA (FH 23 µM + $3.12x10^{-6}$ M CA + $3.4x10^{-7}$ M EDTA), ferrihydrite in the presence of LHA (FH 23 µM + 5% LHA). Mean values □ SE (n = 3) are presented.

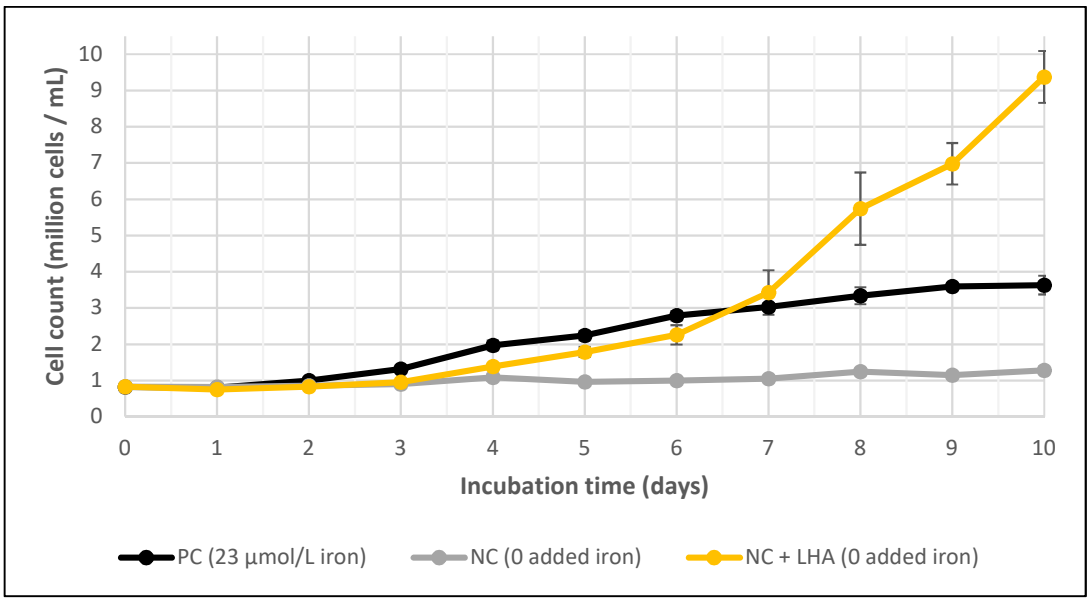

Figure A1.9 Cell number in cultures of *C. vulgaris* containing LHA and varying species and concentrations of iron. Positive control (PC 23 µM ammonium ferric citrate green + $3.12x10^{-6}$ M CA + $3.4x10^{-7}$ M EDTA), negative control (NC, iron-depleted + $3.12x10^{-}$

^{6} M CA + 3.4x10^{-7} M EDTA), negative control containing LHA (NC + 5% LHA). Mean values □ SE (n = 3) are presented.

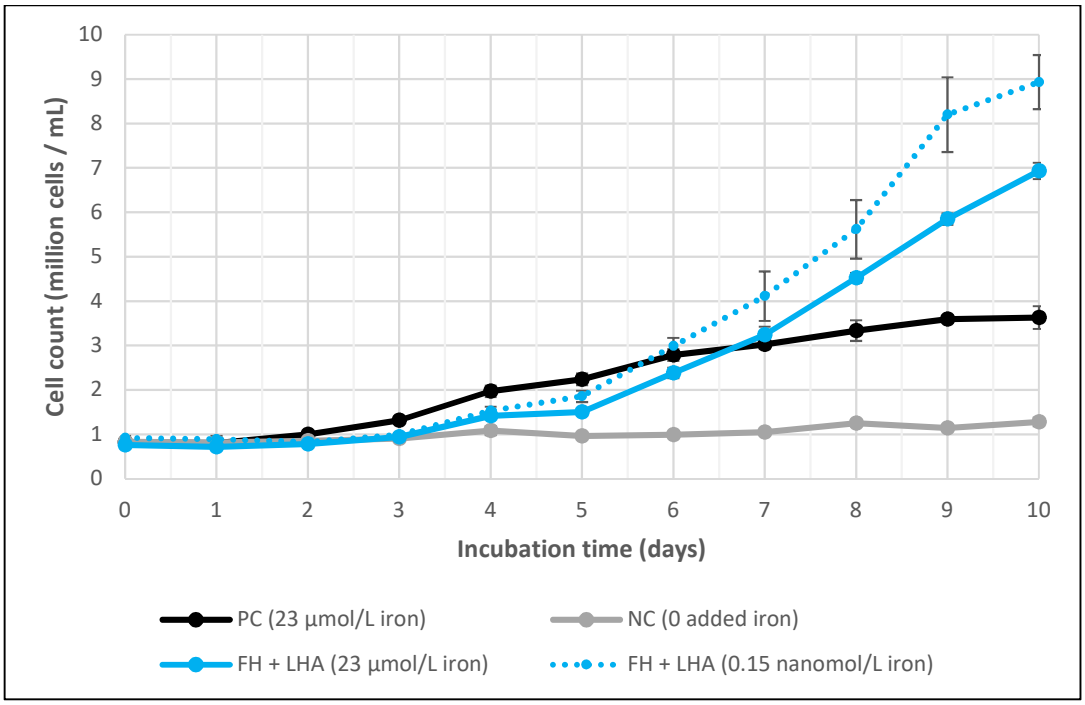

Figure A1.10 Cell number in cultures of *C. vulgaris* containing LHA and varying species and concentrations of iron. Positive control (PC 23 µM ammonium ferric citrate green + 3.12x10^{-6} M CA + 3.4x10^{-7} M EDTA), negative control (NC, iron-depleted + 3.12x10^{-6} M CA + 3.4x10^{-7} M EDTA), ferrihydrite (23 □M) with LHA (FH + 5% LHA) and ferrihydrite (0.15 nM) with LHA (FH + LHA). Mean values □ SE (n = 3) are presented.

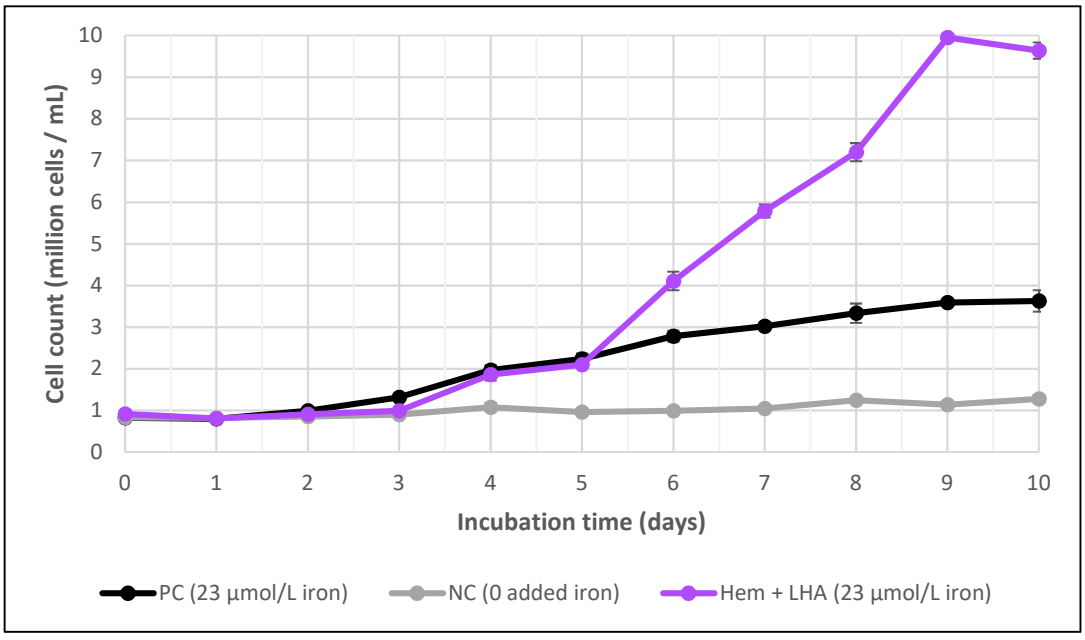

Figure A1.11 Cell number in cultures of *C. vulgaris* containing LHA and varying species and concentrations of iron. Positive control (PC 23 µM ammonium ferric citrate green + 3.12x10^{-6} M CA + 3.4x10^{-7} M EDTA), negative control (NC, iron-depleted + 3.12x10^{-6} M CA + 3.4x10^{-7} M EDTA) and hematite (23 □M) with 5% LHA (Hem + LHA). Mean values □ SE (n = 3) are presented.

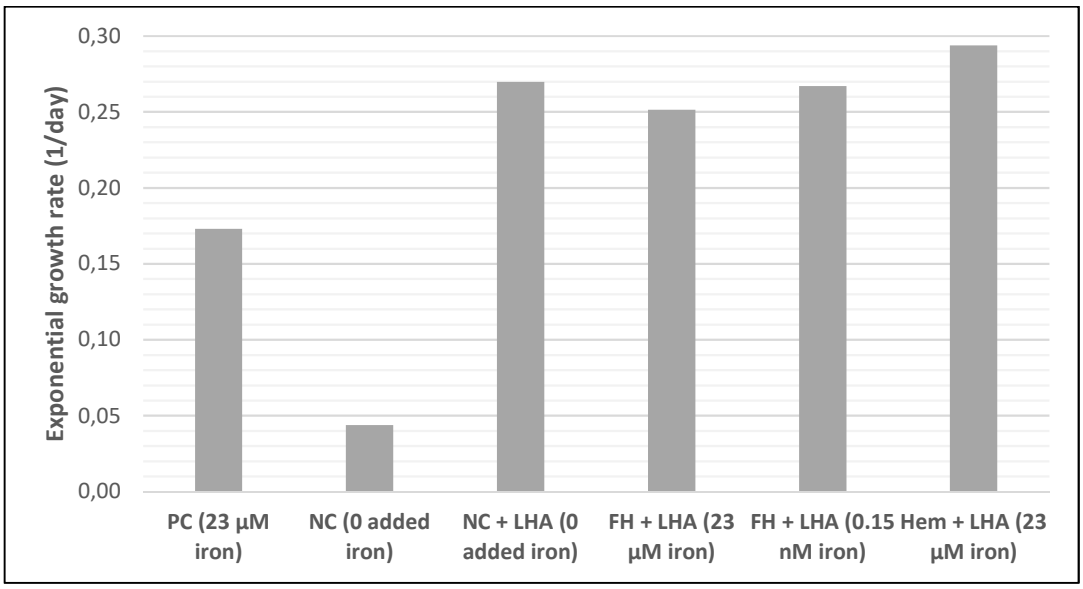

Figure A1.12 Exponential growth rates of *C. vulgaris* cultures containing LHA and varying species and concentrations of iron. Positive control (PC, 23 □M ammonium ferric citrate green + $3.12x10^{-6}$ M CA + $3.4x10^{-7}$ M EDTA), negative control (NC, iron-depleted + $3.12x10^{-6}$ M CA + $3.4x10^{-7}$ M EDTA), negative control with LHA (NC + 5% LHA), ferrihydrite with LHA (23 □M FH + 5% LHA), ferrihydrite with LHA (0.15 nM FH + 5% LHA), and hematite with LHA (23 □M Hem + 5% LHA). Mean values (n = 3) are presented.

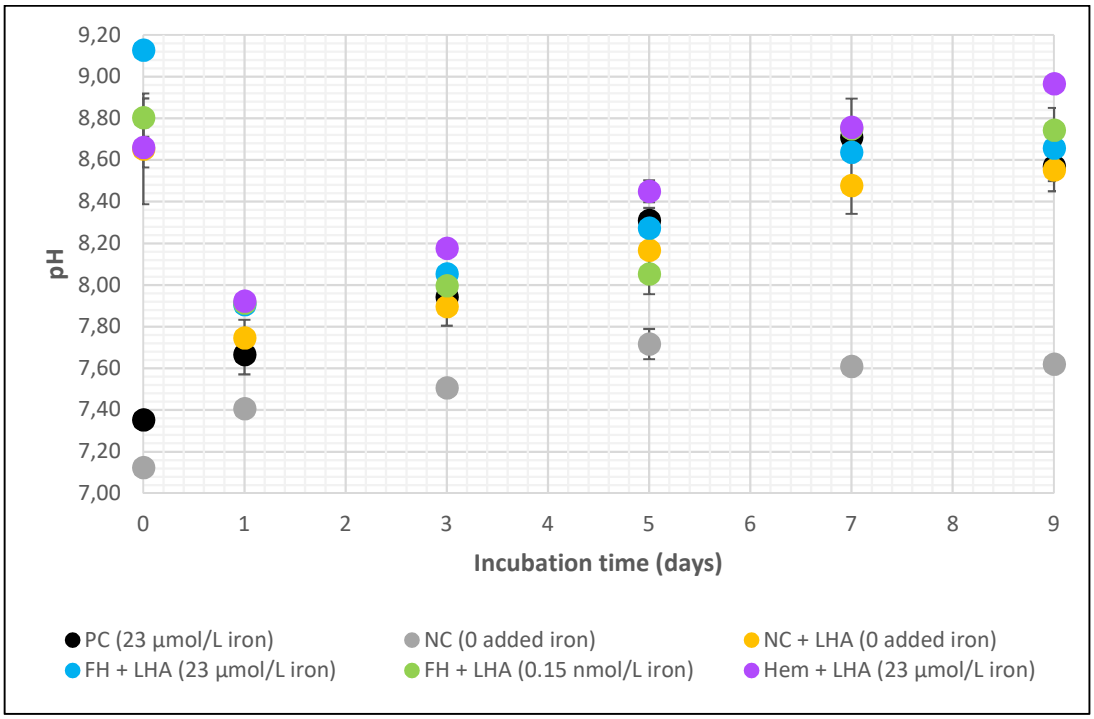

Figure A1.13 pH measurements of *C. vulgaris* cultures containing LHA and varying species and concentrations of iron. Positive control (PC, 23 □M ammonium ferric citrate green + $3.12x10^{-6}$ M CA + $3.4x10^{-7}$ M EDTA), negative control (NC, iron-depleted), negative control with LHA (NC + 5% LHA), ferrihydrite with LHA (23 □M FH + 5% LHA), ferrihydrite with LHA (0.15 nM FH + 5% LHA) and hematite with LHA (23 □M HEM + 5% LHA). Mean values (n = 3) are presented.

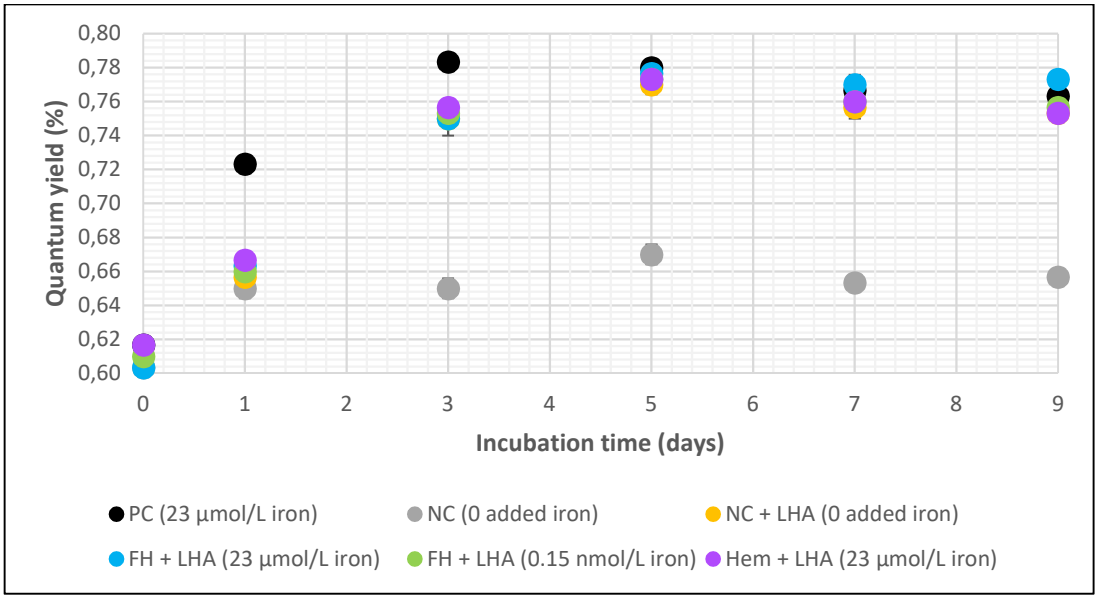

Figure A1.14 Quantum yield of *C. vulgaris* cultures containing LHA and varying species and concentrations of iron. Positive control (PC, 23 □M ammonium ferric citrate green + $3.12x10^{-6}$ M CA + $3.4x10^{-7}$ M EDTA), negative control (NC, iron-depleted), negative control with LHA (NC + 5% LHA), ferrihydrite with LHA (23 □M FH + 5% LHA), ferrihydrite with LHA (0.15 nM FH + 5% LHA), and hematite with LHA (23 □M HEM + 5% LHA). Mean values (n = 3) are presented.

Table A1.15. Cell count measurements for *Pyramimonas* sp. cultures grown at 4°C, in two types of containers (CF = culture flask, EF = Erlenmeyer flask).

Day	CF1 cell count ($x10^3$ cells mL^{-1})	CF2 cell count ($x10^3$ cells mL^{-1})	EF1 cell count ($x10^3$ cells mL^{-1})	EF2 cell count ($x10^3$ cells mL^{-1})
0	313	286	176	192
10	40	79	55	78

Table A1.16. Cell count measurements for *G. theta* cultures under cold conditions, in culture flasks (CF = culture flasks). The result is mean (n = 3) ± SE.

Day	Cell count ($x10^3$ cells mL^{-1})
0	457 ± 8.76
10	NA

Appendix 2

Table A2.1. Calculated and measured iron concentration in samples containing iron and LHA. The results are presented as mean (n = 3) □ SE.

Sample content	Calculated conc. (□M)	Method "A": Filtering, then acidifying – conc. (□M)	Method "B": Acidifying, then filtering – conc. (□M)
$FeCl_3$ with LHA	23	20.03 □ 1.80	18.38 □ 0.21

Ferrihydrite with LHA	23	1.68 □ 0.22	1.54 □ 0.06
Hematite with LHA	23	Below LOD	Below LOD

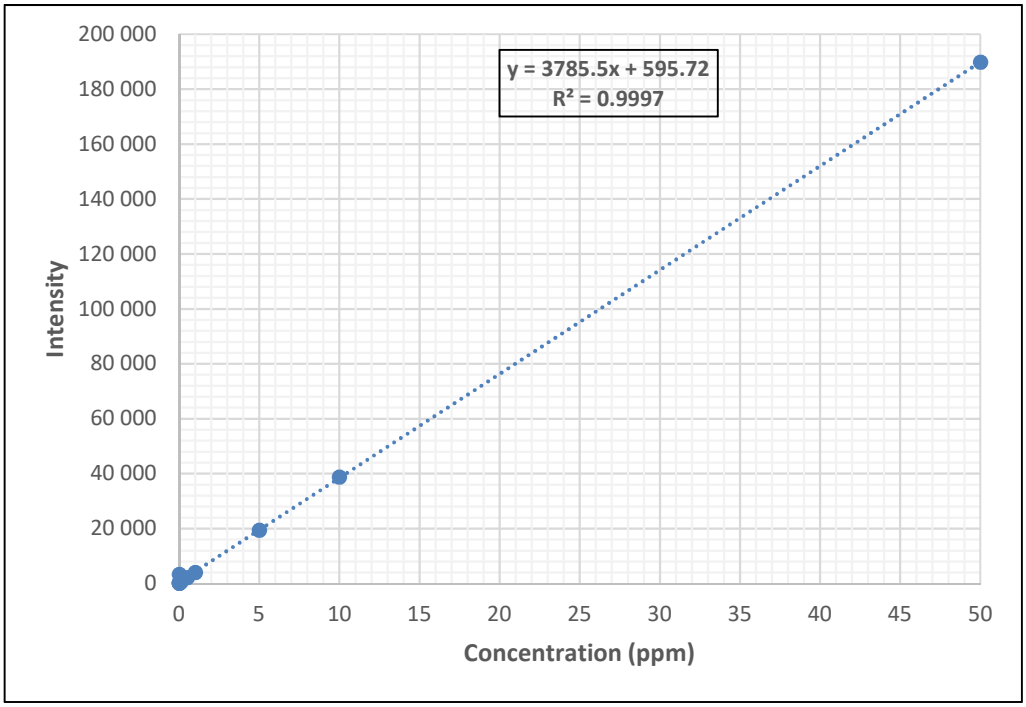

Figure A2.2. Calibration curve for ICP-OES using standards containing iron in known concentrations.

Table A2.3. Iron concentrations at day 0 and day 5 in *C. vulgaris* cultures containing LHA and varying species and concentrations of iron, measured by ICP-OES. Positive control (PC, 23 µM ammonium ferric citrate green + $3.12x10^{-6}$ M CA + $3.4x10^{-7}$ M EDTA), negative control (NC, iron-depleted + $3.12x10^{-6}$ M CA + $3.4x10^{-7}$ M EDTA), negative control containing LHA (NC + 5% LHA), ferrihydrite (23 □M) with LHA (FH + 5% LHA), ferrihydrite (0.15 nM) with LHA (FH + 5% LHA), and hematite (23 □M) with 5% LHA (Hem + LHA). Mean values (n = 3) are presented.

Sample name	Iron type	LHA added	Calculated conc. of iron on day 0 (□M)	Calculated conc. of iron on day 5 (□M)
Positive control	Ammonium ferric citrate green	No	19.53 □ 0.15	0.07 □ 0.06
Negative control	No added iron	No	Below LOD	Below LOD
Negative control + LHA	No added iron	Yes	Below LOD	Below LOD
Fh (23 □M iron) + LHA	Ferrihydrite	Yes	Below LOD	Below LOD
Fh (0.15 nM iron) + LHA	Ferrihydrite	Yes	Below LOD	1.13 □ 0.11
Hem (23 □M) + LHA	Hematite	Yes	Below LOD	1.18 □ 1.03

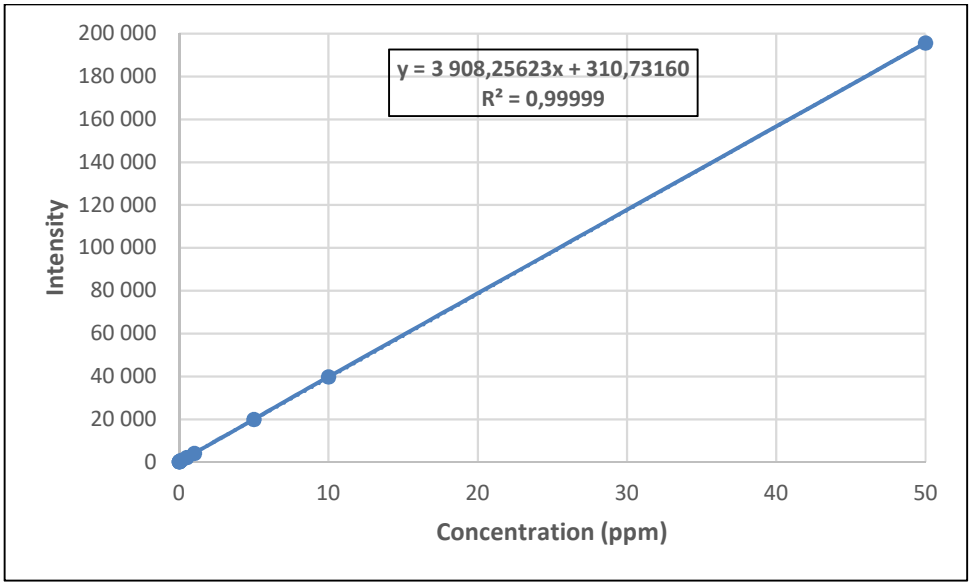

Figure A2.4 Calibration curve for ICP-OES, using standards containing iron in known concentrations.

Figure A2.5 LHA solution after 24 hours of extraction using 12 M HCl.

Table A2.6 Iron concentrations in solutions containing LHA post-extraction, measured using ICP-OES at 238.204 nm wavelength.

Extraction method / dilution factor	**Concentration of iron (µM)**
1M HCl / x10	1.563
1M HCl / x100	1.780
1M HCl / x1,000	2.339
Water / x100	83
Water / x1,000	248
Water / x10,000	1.179
12M HCl / x100	21
12M HCl / x1,000	147
12M HCl / x10,000	1.868

Appendix 3

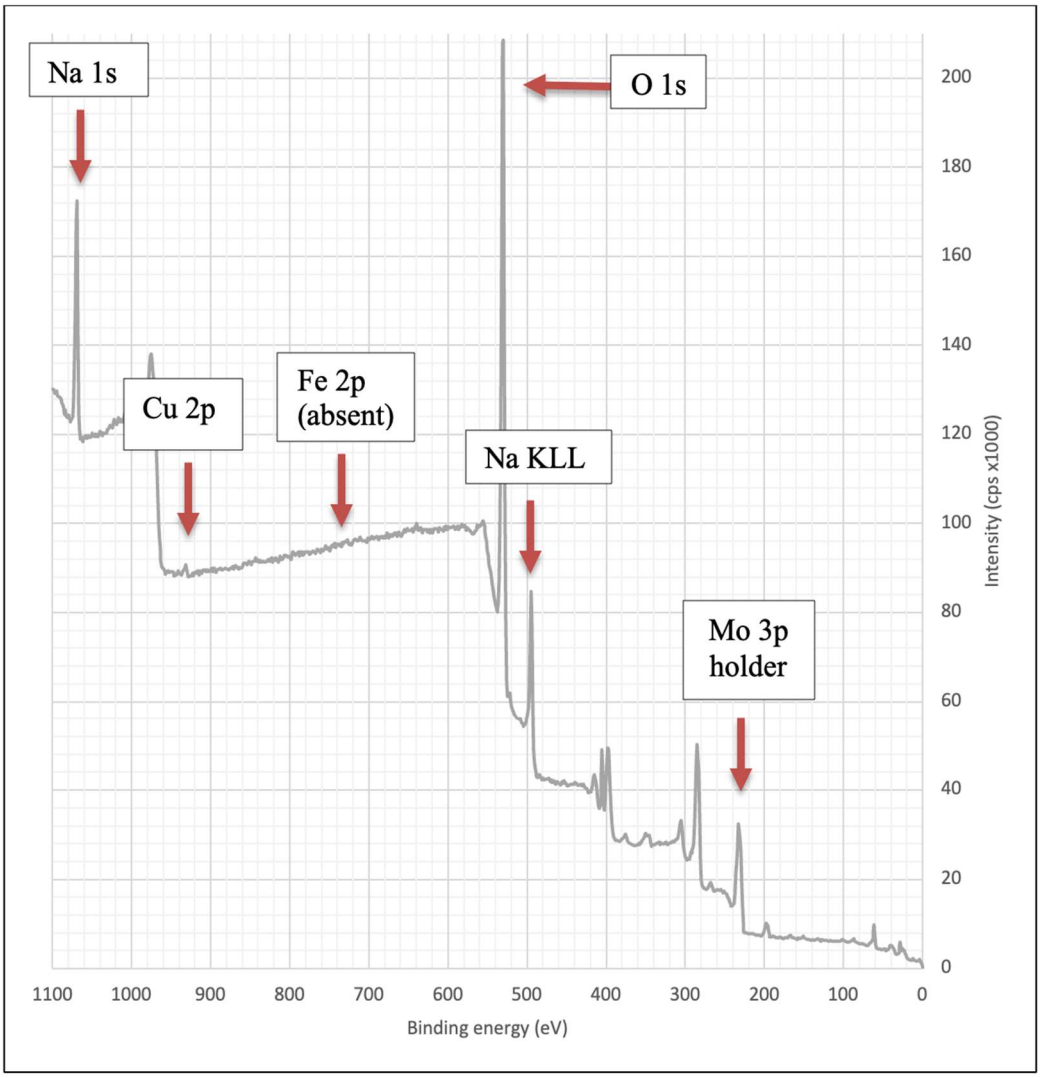

Figure A3.1 XPS analysis performed on a *C. vulgaris* culture grown for 10 days in the presence of LHA and ferrihydrite.

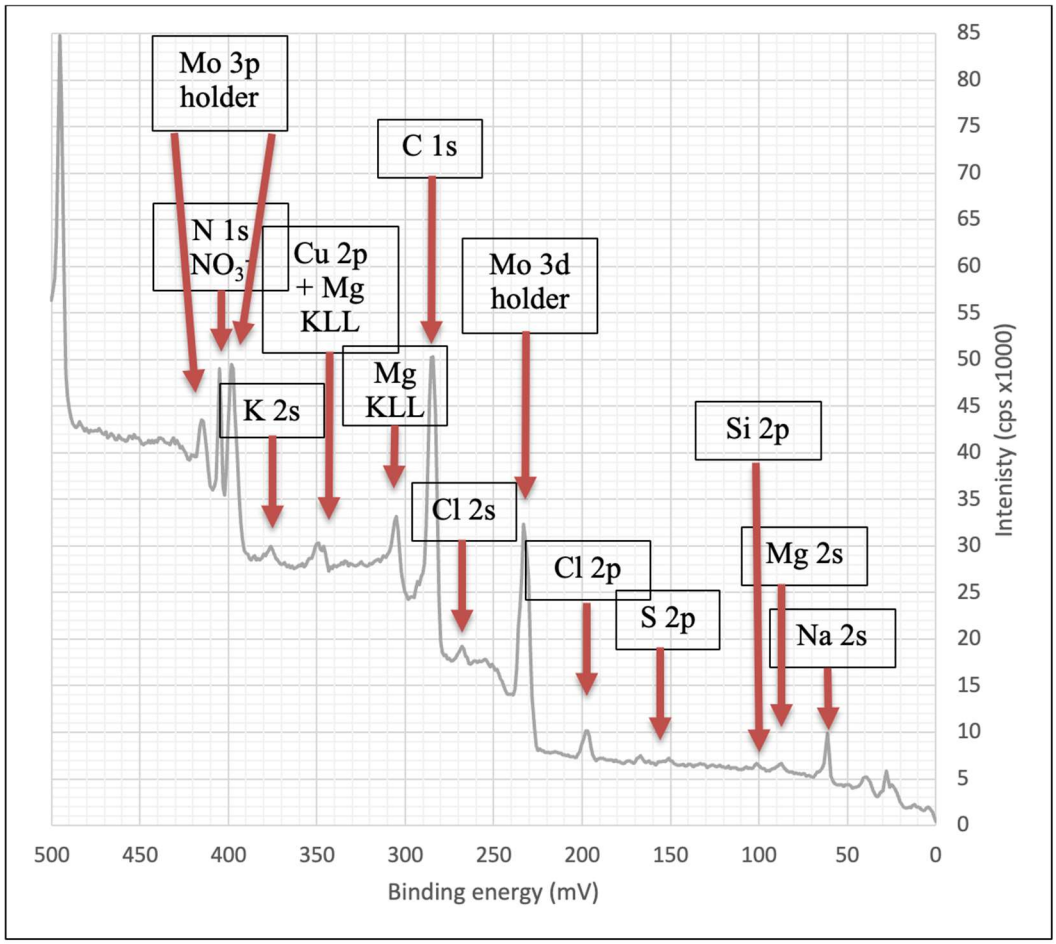

Figure A3.2 XPS analysis performed on a *C. vulgaris* culture grown for 10 days in the presence of LHA and ferrihydrite (close up at binding energy values 0 - 500 mV).

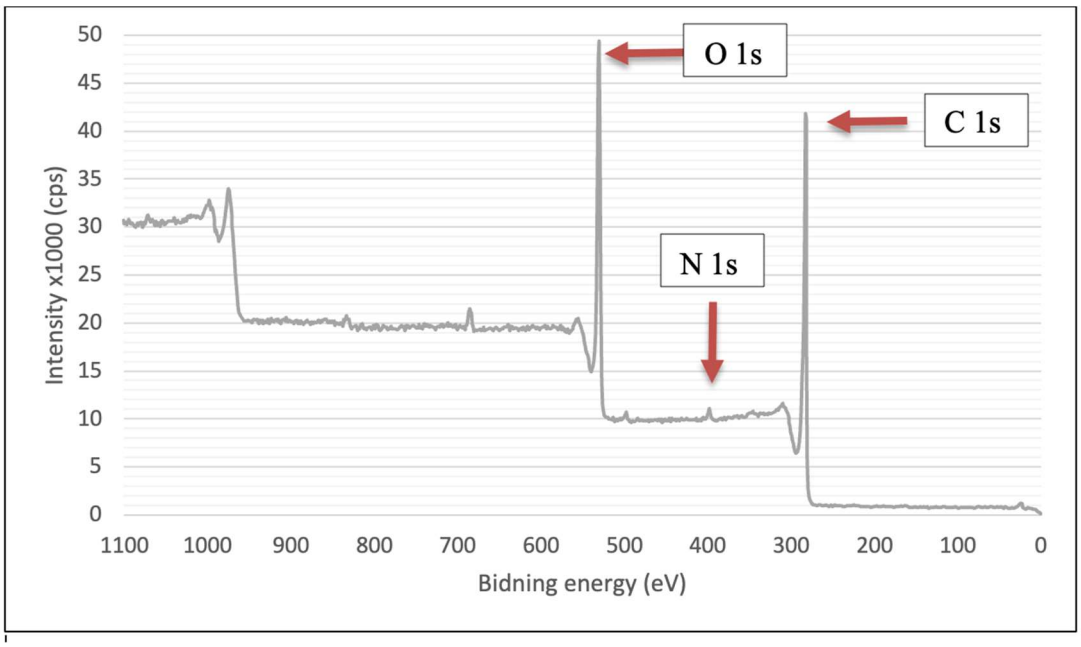

Figure A3.3 XPS analysis performed on a sample of LHA standard.

Table A3.4 Binding energy values that correlate to specific elements and orbitals (as presented in **Figures A3.1-A3.3**)

Binding energy range (eV)	Species
64	Na 2s
89	Mg 2s
102	Si 2p
164-165	S 2p
199-201	Cl 2p
228-231	Mo 3d (holder)
271	Cl 2s
282.31-285.04	C 1s
301	Mg KLL
347-351 ,347	Ca 2p + Mg KLL
380	K 2s
398	N 1s (NO_3^-)
394-412	Mo 3p (holder)
493	Na KLL
531	O 1s
707-720	Fe 2p
347-351	Ca 2p
1072	Na 1s

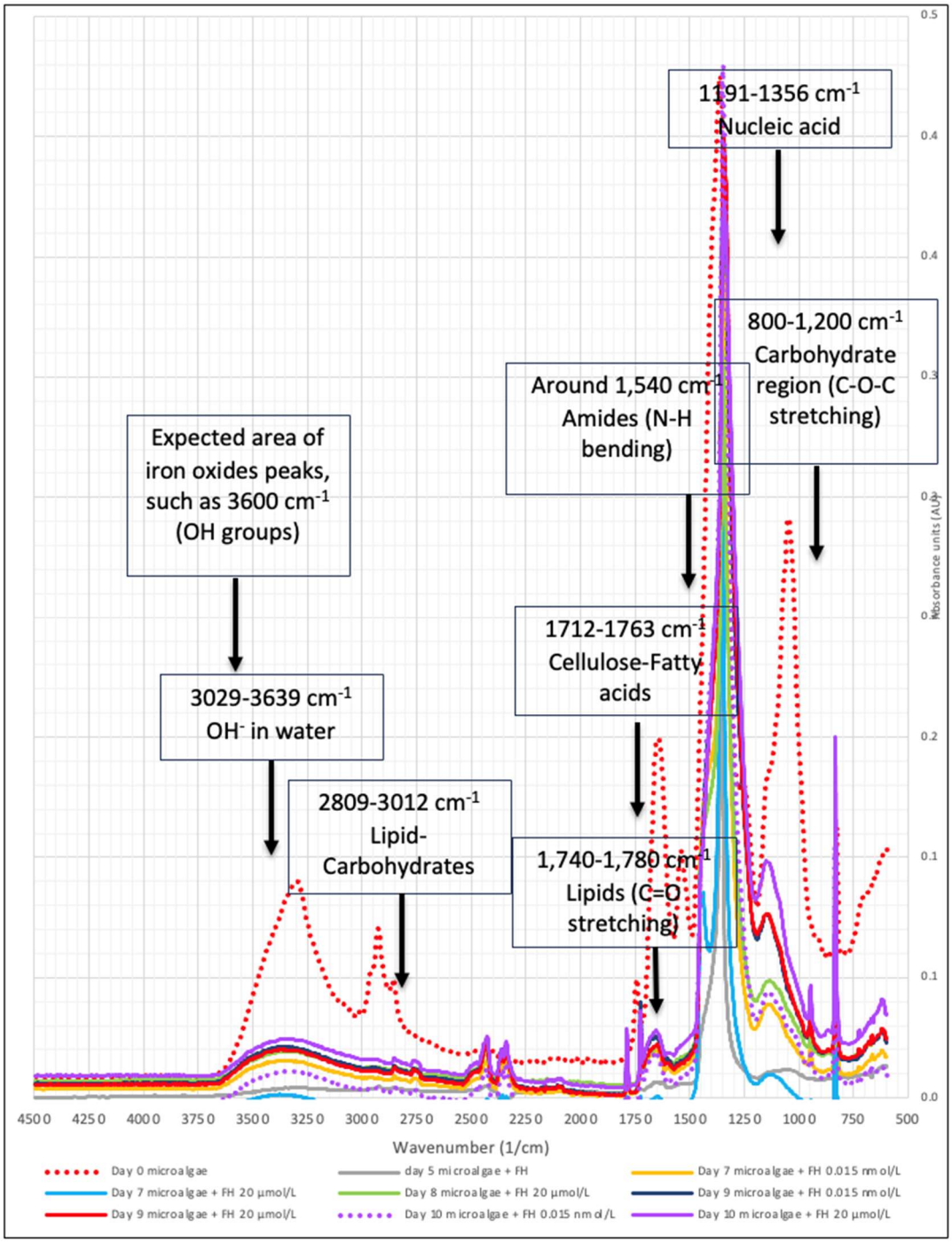

Figure A3.5. FTIR spectra of *C. vulgaris* cultures grown in the presence of ferrihydrite. Spectral peaks characteristic for *C. vulgaris*[39] and expected areas for iron oxide[40] are assigned.

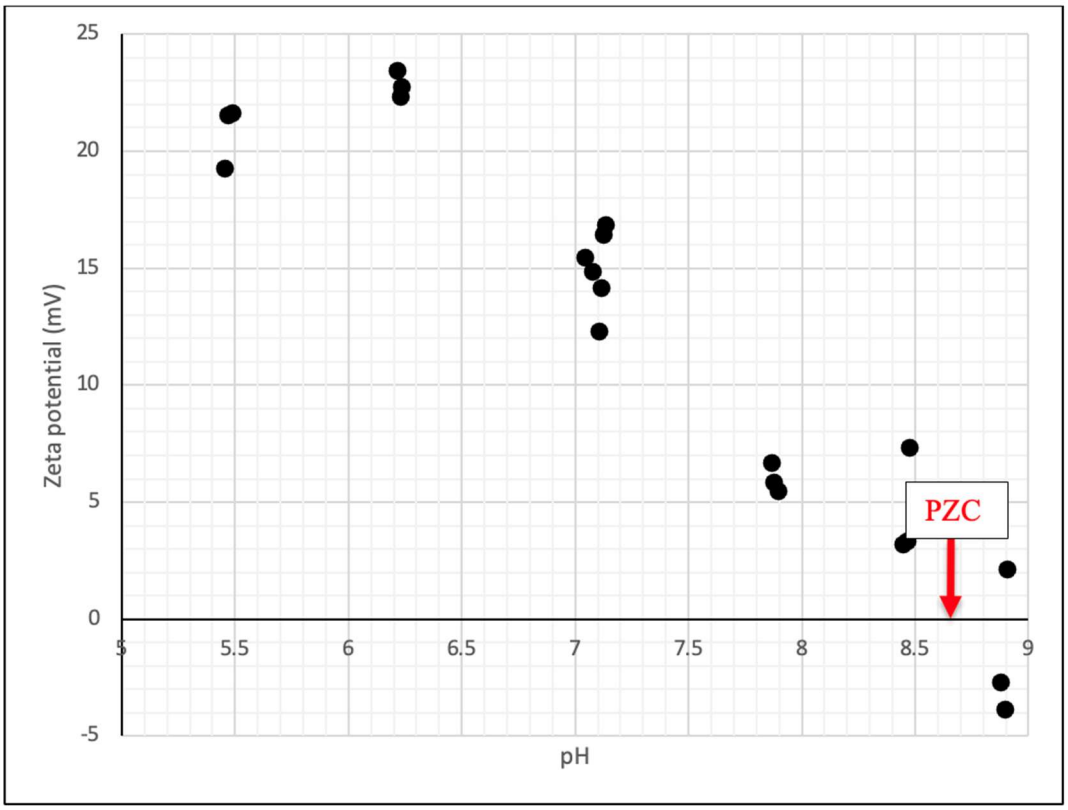

Figure A3.6 Zeta potential measurement of ferrihydrite nanoparticles at different pH values. The PZC (point of zero charge) is marked by a red arrow.

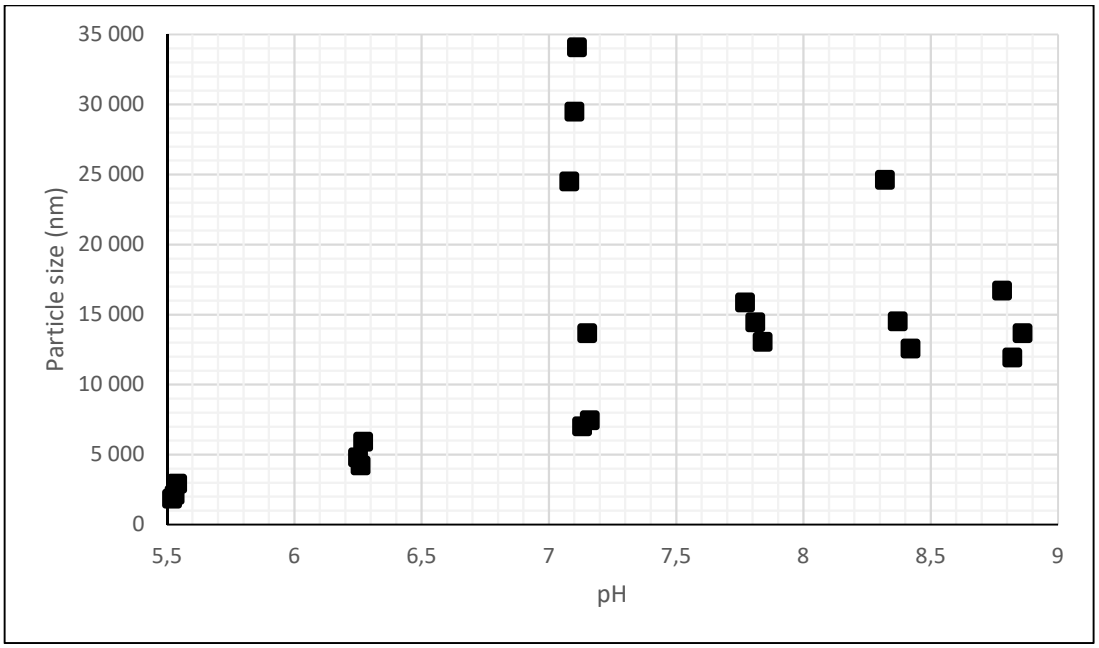

Figure A3.7 Particle size measurement of ferrihydrite nanoparticles at different pH values.

Appendix 4

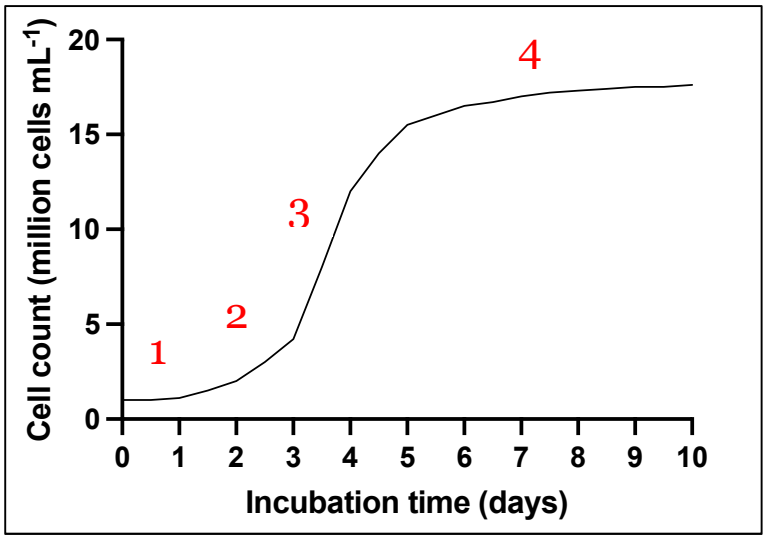

Figure A4.1 Growth plot of microalgae culture where cell count numbers are plotted against incubation time (1 – lag phase, 2 – exponential phase, 3 – linear phase, 4 – stationary phase, followed by the death phase which is not shown in the figure)

Table A4.2 Comparison between $Q_{0.05}$ and Q_{calc} values that were calculated for the purpose of performing Tukey's test on the results of microalgae culture cell counts in the presence and absence of LHA.

First treatment	Second treatment	$Q_{0.05}$	Q_{calc}
Negative control	Negative control + LHA	4.90	12.6
Negative control	23 □M ferrihydrite and LHA	4.90	8.80
Negative control	23 □M hematite and LHA	4.90	13.02
Negative control	0.15 nM ferrihydrite and LHA	4.90	8.80
Positive control	23 □M ferrihydrite and LHA	4.90	5.15